Science of the Total Environment 671 (2019) 388–403

Contents lists available at ScienceDirect

Science of the Total Environment

journal homepage: www.elsevier.com/locate/scitotenv

Review

Reduction of nitrate by zero valent iron (ZVI)-based materials: A review

Yong Liu [a,b], Jianlong Wang [b,c,*]

[a] College of Chemistry and Materials Science, Sichuan Normal University, Chengdu 610066, PR China
[b] Collaborative Innovation Center for Advanced Nuclear Energy Technology, INET, Tsinghua University, Beijing 100084, PR China
[c] Beijing Key Laboratory of Radioactive Wastes Treatment, Tsinghua University, Beijing 100084, PR China

HIGHLIGHTS

- The recent advances in nitrate reduction by ZVI-based materials were reviewed.
- The effect of ZVI characteristics on nitrate reduction was discussed in detail.
- The effect of operational parameters on nitrate reduction by ZVI was summarized.
- The nitrate reduction by ZVI alone usually leads to the formation of ammonium.
- The modification strategies of ZVI to improve N_2 selectivity were introduced.

GRAPHICAL ABSTRACT

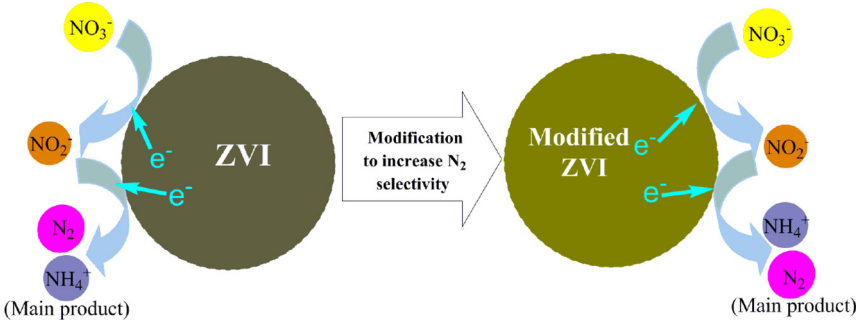

ARTICLE INFO

Article history:
Received 6 February 2019
Received in revised form 14 March 2019
Accepted 20 March 2019
Available online 26 March 2019

Editor: Jay Gan

Keywords:
Nitrate
Iron
Water treatment
Denitrification
Nitrate reduction

ABSTRACT

Zero valent iron (ZVI) and ZVI-based materials have been widely used for the reduction of nitrate, a major contaminant commonly detected in groundwater and surface water. The reduction of nitrate by ZVI is influenced by various factors, such as the physical and chemical characteristics of ZVI and the operational parameters. There are some problems for the nitrate reduction by ZVI alone, for example, the formation of iron oxides on the surface of ZVI at high pH condition, which will inhibit the further reduction of nitrate; in addition, the end reduction product is mainly ammonium, which itself needs to be concerned. Several strategies, such as the optimization of the structure of ZVI composites and the addition of reducing assistants, have been proposed to increase the reduction efficiency and the selectivity of end product of nitrate reduction in a wide range of pH, especially under neutral pH condition. This review will mainly focus on the high efficient reduction of nitrate by ZVI-based materials. Firstly, the reduction of nitrate by ZVI alone was briefly introduced and discussed, including the influence of physical and chemical characteristics of ZVI and some operational parameters on the reduction efficiency of nitrate. Then, the strategies for enhancing the reduction efficiency and the N_2 selectivity of the reductive products of nitrate were systematically analyzed and evaluated, especially the optimization of the structure of ZVI composites (e.g., doped ZVI composite, supported ZVI composite and premagnetized ZVI), and the addition of reducing assistants (e.g., metal cations, ligand, hydrogen gas and light) were highlighted. Thirdly, the mechanisms and pathways of nitrate reduction were discussed. Finally, concluding remarks and some suggestions for the future research were proposed.

* Corresponding author at: Energy Science Building, INET, Tsinghua University, Beijing 100084, PR China.
E-mail address: wangjl@tsinghua.edu.cn (J. Wang).

https://doi.org/10.1016/j.scitotenv.2019.03.317
0048-9697/

Contents

1. Introduction

Nitrate is one of the nitrogen compounds with high solubility in aqueous solutions. More and more attentions have been paid to nitrate contamination in groundwater and surface water from the fertilizers, livestock manure, the industrial and domestic wastewater, and so on. Nitrate pollution can cause some environmental problems, such as eutrophication and serious human health problems (Tugaoen et al., 2017; Shen and Wang, 2011). Therefore, it is necessary to remove nitrate from water and wastewater.

Various methods have been developed and applied for the removal of nitrate from aqueous solutions, including biological denitrification, chemical reduction, ion exchange, adsorption, and membrane separation such as reverse osmosis process (Wu et al., 2018; Wang and Chu, 2016). Ion exchange, adsorption, and membrane processes only separate nitrate from aqueous solutions and will produce exhausted resins and adsorbents, and concentrated nitrate rejection (Kapoor and Viraraghavan, 1997; Tugaoen et al., 2017). Biological treatment process usually requires external supplementation of organic substances to generate dedicated microbial communities and provide [H] or exogenous electron donors for nitrate reduction when intrinsic organic substances in wastewater are insufficient. Moreover, biological denitrification tends to be a time-consuming process, and a lot of biological sludge are produced during the denitrification process, which need further disposal.

The chemical reduction based on some inorganic electron donors is becoming increasingly attractive due to its easy operation and high efficiency. Several inorganic electron donors have been reported to reduce or eliminate nitrate (Kapoor and Viraraghavan, 1997; Shen and Wang, 2011). Among them, zero valent metals, such as zero valent aluminum (Zhao et al., 2014), zero valent magnesium (Ramavandi et al., 2011) and zero valent zinc (Liou et al., 2012) have been used for reducing nitrate from aqueous solution due to their strong reduction performance, easy to operation, and the simple maintenance of the reduction process.

Zero valent iron (ZVI) is a reactive metal with standard redox potential ($E^0 = -0.44$ V), which is abundant and cheap (Ezzatahmadi et al., 2017; Wang and Bai, 2017). It is thus an effective and widely used reducing agent for the removal of nitrate from groundwater and wastewater. The main concerns for the reduction of nitrate by ZVI include the directional transfer of electron from ZVI to nitrate, which transforms nitrate into low valence inorganic nitrogen species, as well as the dissolution of ZVI to form soluble ionic products or insoluble oxide. The reduction efficiency of nitrate is affected by the physical and chemical characteristics of ZVI, as well as the operational parameters. In order to keep nitrate being reduced by ZVI at an appropriate rate, it is necessary to enhance iron corrosion and to dissolve ferrous oxides on the surface of ZVI. To accomplish this, adding acid solution during the reduction of nitrate by ZVI is the most commonly used method (Huang and Zhang, 2004). However, the addition of acid solution will decrease the pH value and increase the content of anions in the effluent, which will cause potential risks for the human health during the denitrification of groundwater for the drinking water and will pose serious threat to eco-environmental safety during the denitrification of wastewater. Moreover, adding acid solution is not convenient and not practical for use. Therefore, some strategies have been used to promote nitrate reduction efficiency by ZVI, especially under near-neutral or neutral conditions (Kamarehie et al., 2018; Eljamal et al., 2018; Yun et al., 2018). These strategies can be roughly divided into two categories. One is the optimization of the chemical composition and structure of ZVI composites; the other is the addition of reduction assistants. The enhancing reduction efficiency of nitrate by the first strategy is owing to that, the optimized ZVI composites have the following performances: (1) to change electron transfer pathway; (2) to increase the transfer rates of electron and mass; (3) to reduce the overlap of active site on the surface of ZVI composite by iron oxides; and (4) to provide some buffer capability. The related strategies were to use doped ZVI composites, supported ZVI composites and premagnetizated ZVI composites,

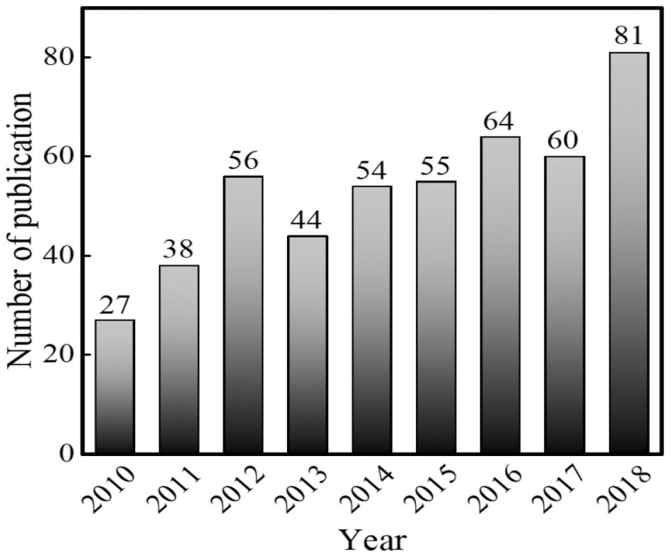

Fig. 1. Number of publications on ZVI and nitrate over the past nine years.

etc. In second strategy, augmenting promoter, such as ferrous ion and ligand or augmenting additional reducing agents, such as hydrogen and photoelectron are used to facilitate the reduction of nitrate by ZVI. Compared with ZVI alone, the nitrate reduction efficiency could be facilitated, especially under near-neutral or neutral conditions by above strategies. However, the main reduction product of nitrate over ZVI and ZVI composites is ammonia, which is also a contaminant required to be removed from aqueous solution. As a result, many studies have concentrated on seeking solutions to convert nitrate to nitrogen gas (N_2) by ZVI (Lubphoo et al., 2015; Teng et al., 2017; Zhang et al., 2019). These solutions are similar to the strategies for promoting nitrate reduction efficiency. For example, the nitrate reduction by supported bimetallic Fe—Pd nanoparticles at pH 6.75 could gain N_2 selectivity of 69.2% (Shi et al., 2016). More than 82% of the N_2 selectivity was obtained at an initial solution pH of 4 when nitrate reduction was proceeded by Cu–nZVI/TiO_2 composite under UV irradiation (Krasae and Wantala, 2016). Therefore, how to further enhance nitrate reduction efficiency and N_2 selectivity is a very urgent issue. Fig. 1 shows the number of papers in recent years about the nitrate reduction by ZVI-based on the database of web of sciences using “nitrate reduction” and “zero-valent iron” as key words. It can be seen that nitrate reduction by ZVI becomes more and more attractive in recent years.

In order to understand the strategies for enhancing nitrate reduction by ZVI, this review will address several relevant issues, including the influence of physical and chemical characteristics of ZVI and operational parameters on the reduction efficiency of nitrate by ZVI alone, the strategies of using ZVI composites for nitrate reduction, the nitrate reduction mechanisms by ZVI composites, and the strategies of addition of reduction assistants to ZVI to increase the reduction efficiency of nitrate, especially under near-neutral or neutral pH conditions. The reduction product of nitrate by ZVI composites was also summarized and analyzed. The thorough review of these aspects would help readers to explore potential possibilities of ZVI for nitrate reduction and provide a direction for the development of ZVI-based materials in the future.

2. Influence of different factors on nitrate reduction by ZVI alone

2.1. Physical and chemical characteristics

According to the size of particles, ZVI can be divided into micro-scale zero valent iron (mZVI) and nano-scale zero valent iron (nZVI). There is a significant difference in the reduction efficiency of nitrate between mZVI particles and nZVI particles due to their difference of size. It is well established that particles with smaller size will have greater effective surface area, which show higher reductive efficiency (Choe et al., 2000). Therefore, the activity of nZVI particles is often higher than that of mZVI particles. For example, nitrate concentration was almost unchanged in 2 h by mZVI in commercial iron powders, while nitrate was completely disappeared in 0.5 h by nZVI particles (80 nm) with same amount of mZVI particles (Wang et al., 2006).

As for nZVI particles, physical characteristics are determined by their preparation methods. Table 1 shows the relationship between the preparation methods and physical characteristics of nZVI particles. The size and specific surface area of most nZVI particles used for the nitrate reduction are in the range of 1–100 nm and 20–60 m^2/g, respectively. The surface morphology of nZVI particles includes flower-like shaped highly dispersed nZVI particles (Ghosh et al., 2017), spherical nanoparticles (Wang et al., 2006), crystalline rod/needle-like nZVI particles (Liu et al., 2012), quasi spherical amorphous nZVI particles (Wang et al., 2014), chain like nZVI particles (Ghosh et al., 2017), and so on. The preparation methods of ZVI have significant influence on the size, specific surface area and surface morphology of nZVI particles (Stefaniuk et al., 2016). The preparation methods of nZVI particles include ferrous iron reduction by borohydride (Khalil et al., 2018; Kim et al., 2012; Lu et al., 2016; Wang et al., 2006), arc discharge (Kassaee et al., 2011), combining electrochemical and ultrasonic methods (Chen et al., 2004), and hydrogen reduction of goethite (Liu et al., 2012), and so on. nZVI particles are usually obtained by borohydride reduction of a ferrous iron solution. The conditions of the borohydride reduction, such as reaction media, the mass ratio of borohydride to ferrous iron, reaction time will also affected the performance of nZVI particles, such as size, specific surface area and surface morphology. For example, the nZVI particles obtained by $NaBH_4$ reduction in ethanol–water mixed solvent in the presence of dispersion agent of polyglycol were spherical particles with higher surface area (80 nm, 54.25 m^2/g), while the lower surface area particle (80 nm, 8.08 m^2/g) was obtained with only de-ionized water as reaction media (Wang et al., 2006). Moreover, the composition of nZVI particles was also affected by the preparation method. For instance, the nZVI particles prepared by arc discharge reduction were pure ZVI, while the nZVI particles produced via the reduction of $FeSO_4$ by $NaBH_4$ contained an impurity of Fe_3O_4 (Kassaee et al., 2011). The nZVI particles were produced by combining electrochemical and ultrasonic methods contained an impurity of Fe_2O_3 (Chen et al., 2004). Compared with nZVI particles produced by hydrogen reduction of hydrothermal goethite, the nZVI particles produced by hydrogen reduction of natural goethite contained some Al-substitution (Liu et al., 2012).

The performance of nZVI particles for the nitrate reduction was affected more by their crystal phase purity rather than their size. For example, nZVI particles (37 nm) produced by arc discharge reduction showed two-fold efficiency than that of nZVI particles (30 nm) produced via the reduction of $FeSO_4$ by $NaBH_4$ (Kassaee et al., 2011), because the arc fabricated nZVI particles had higher purity. In another example, three types of nZVI particles were synthesized by using three different alcohol-water mixture, i.e., ethanol-water (Eth-NP), ethylene glycol-water (Eth-gly-NP) and glycerol-water (Gly-NP). The Eth-NPs particles were smallest in dimension (5–10 nm), whereas Gly-NP particles were largest in size (50–100 nm). Interestingly, Gly-NP particles with large particle size showed highest removal efficiency (100%) within 2 h, and Eth-NPs particles showed lowest activity (70%) within 2 h. Gly-NPs particles and Eth-gly-NP particles were pure ZVI, while Eth-NP particles had an impurity of Fe_3O_4 (Ghosh et al., 2017). Therefore, it seemed that the purity of nZVI particles played an important role in the reduction activity of nZVI. Moreover, the resistance to oxidation of nZVI could also affect its reactivity, stability, and transformation capability (Sohn et al., 2006).

It has been proved that mZVI particles can reduce nitrate to ammonia almost completely. However there are different results on the reduction product of nitrate by nZVI particles. Most scholars found that the

Table 1
Main physical characteristics, preparation methods and reduction activity of ZVI for the removal of nitrate.

Size	Specific surface area (m^2/g)	Morphology	Preparation methods	ZVI dosage (g/L)	NO_3^- concentration (mg/L)	Time (h)	Initial pH ≤ 4 (%)	Reduction at near-neural pH (%)	Reduction products	Reference
6 ± 10 mm	0.31	–	–	20	50	0.5	95	Negligible	100% NH_4^+	(Huang et al., 1998)
20–60 mesh	~1.1	–	–	>4000	130	24	~100	50	100% NH_4^+	(Suzuki et al., 2012)
10–40 nm	14.5	Rod-like and needle- like crystals	Hydrogen reduction of natural goethite	3.2	80	5	95.5	90	N_2, 20% NH_4^+, a little NO_2^-	(Liu et al., 2012)
–	–	Spherical and form chain-like clusters	Fe^{2+} reduction by $NaBH_4$	3.2	130	10	–	>95	95% NH_4^+	(Kim et al., 2012)
20–80 nm	–	Quasi-spherical	Fe^{2+} reduction by green tea	1	20	–	–	51.7	–	(Wang et al., 2014)
~80 nm	54.25	Spherical	Fe^{2+} reduction by KBH_4 in ethanol–water mixed solvent.	4	350	0.5	–	100	Main NH_4^+	(Wang et al., 2006)
~37 nm	–	Dispersed spheres	Arc discharge vs. reduction	1.33	30	24	54	<20	–	(Kassaee et al., 2011)
1–20 nm	25.4	–	Combining electrochemic- al and ultrasonic methods	0.5	88	4	78	50.	36.2–45.3% NH_4^+	(Chen et al., 2004)
~90 nm	65.74	Well-dispersed single phasic flower-like	Fe^{3+} reduction by boro-hydride using glycerol- water as solvents.	2.88	400	2	–	100	>99% NH_4^+	(Ghosh et al., 2017)
~70 nm	–	Round shaped with flaky materials	Fe^{3+} reduction by borohydride using ethylene glycol-water	2.88	400	2	–	~88	>99% NH_4^+	(Ghosh et al., 2017)
~20 nm	–	Agglomerated round shaped forming chain-like structure	Fe^{3+} reduction by boro-hydride using ethanol-water as solvents	2.88	400	2	–	~72	>99% NH_4^+	(Ghosh et al., 2017)

reduction product of nitrate by nZVI particles was mainly ammonia (Ryu et al., 2011; Li et al., 2018; Yang et al., 2018). However, some researchers found that reduction product of nitrate by nZVI particles contained 10–45% ammonia or 100% N_2 (Chen et al., 2004). The low ammonia in the reduction product of nitrate by nZVI particles was mainly due to that nitrate was converted to ammonium ion followed by ammonia stripping under a strong alkaline condition, leading to a decrease in the total aqueous nitrogen amount (Hwang et al., 2011).

2.2. Operational parameters

There are many factors influencing the reduction of nitrate by ZVI. In addition to the physical and chemical characteristics of ZVI, which was discussed in Section 2.1, some operational parameters, including solution pH, temperature, concentration of dissolved oxygen (DO), and concentration of nitrate and other water quality constituents, can also influence ZVI reactivity, and ultimately affect the fate of nitrate. These influencing factors will be discussed in detail in the following sections.

2.2.1. Effect of pH

The pH of the aqueous solution is an important parameter that will strongly affect the rate of nitrate reduction by ZVI, mainly due to that: (1) nitrate reduction requires the participation of protons; (2) pH greatly affects the rate of ZVI corrosion; (3) pH greatly affects the product of ZVI corrosion (Chen et al., 2004), which was explained by Fig. 2. Considering that the concentration of nitrate in most of researches was over 50 mg/L. A potential - pH predominance area diagram based on thermodynamic theory and the data for the solid of Fe, Fe_2O_3 and Fe_3O_4 is shown in Fig. 2, assuming that total dissolved iron concentration is 1×10^{-2} mol/L.

Fig. 2 shows that the existing form of iron species depended on pH and oxidation-reduction potential (ORP). Fe^{2+} occurs on lower pH and ORP, Fe_2O_3 occurs on higher pH and ORP, Fe_3O_4 occurs on high pH and low ORP. When nitrate reduction was performed without pH-control or buffering solution, the iron oxide would be formed when solution pH rose to neutral or alkaline, which would inhibit electron transfer from ZVI to nitrate.

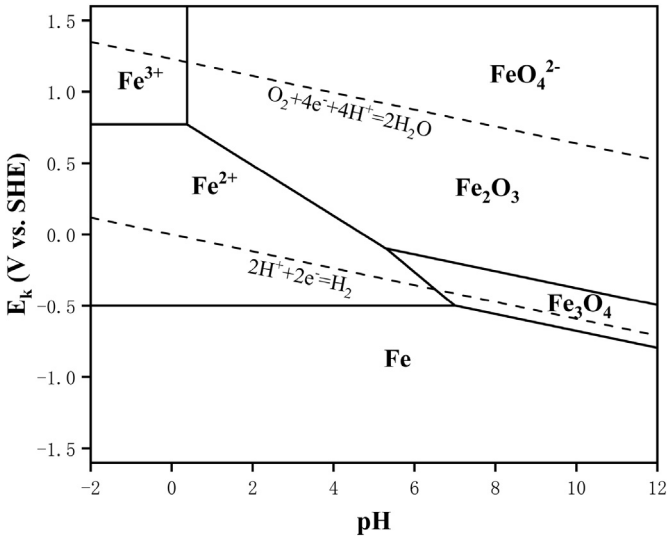

Fig. 2. Pourbaix diagram based on solid species of Fe^0, Fe_2O_3 and Fe_3O_4, assuming that total dissolved iron concentration is 1×10^{-2} mol/L. Dashed lines indicate standard reduction potentials for labeled reactions.

As for both mZVI particles and nZVI particles, the rate constant increased with decrease of pH for the reductive removal of nitrate (Zawaideh and Zhang, 1998; Alowitz and Scherer, 2002). For example, over pH range from 2.5 to 4.5, the reduction rate constant of nitrate by mZVI decreased with increasing pH (Huang and Zhang, 2004). Likewise, Rodríguez-Maroto et al. (2009) revealed that complete reduction of nitrate was obtained in a few hours when pH value was below 2.5, whereas only about 37% of nitrate was reduced after 22 d at pH of 4. Another example for nZVI particles, at initial pH 5, about 80% of nitrate (100 mg/L) could be reduced in solution within 60 min by 2 g/L nZVI, while a complete removal of nitrate by nZVI was obtained after 30 min at pH 4 and even lower pH values (Yang and Lee, 2005). In summary, the good performance of ZVI at low pH may be mainly ascribed to the acceleration of iron corrosion to generate fresh active sites and dissolution of the passivated oxide layers on ZVI surface to improve electron transfer from ZVI to nitrate, while a high pH deteriorated the performance of ZVI due to more iron oxides on the surface of the incorporated ZVI, which inhibited the mass transfer. However, lowering solution pH to very acidic condition (e.g., below 2) may also diminish the nZVI performance, as it can cause the quick dissolution of ZVI into the bulk solution, resulting in an insufficient surface area for the release of Fe^{2+} and less electrons to nitrate. For example, the reduction of nitrate by mZVI decreased from 72% to 60% when initial pH decreased from 1.92 to 1.22 (Zhang et al., 2017).

The influence degree of pH on the reactivity of ZVI depends on the initial pH and ZVI size. Huang et al. (1998) reported that pH effect was not significant for the initial pH of 2–4 during nitrate reduction with 6–10 μm ZVI particles when the solution pH was maintained unchanged. Kim et al. (2016) also reported that pH effect was not significant for initial pH of 3–7, because there was a rapid increase of pH, as a result of OH^- production via the anaerobic corrosion of nZVI particles. The pH level remained at 10.13 ± 0.11 after 15 min, regardless of the initial pH values. Moreover, the effect of pH on the reaction rate is less for nZVI particles than mZVI particles. For example, after 60 min of reaction, the conversion of nitrate (100 mg/L) by mZVI particles decreased drastically from 95% to 0% when initial pH increased from 2.5 to 5 (Huang et al., 1998), while the conversion of nitrate by nZVI particles decreased slightly from 100% to 80% at the same pH conditions (Yang and Lee, 2005). A reasonable explanation for this may be that the formation of iron oxides on the surface of mZVI particles is often faster than nitrate reduction, which leads to the formation of more iron oxides, hindering the transfer of electron at high pH solution. Thus, the nitrate reduction by mZVI particles is pH-dependent, and low pH is favorable for the reduction. As for nZVI particles, the process of nitrate reduction is acid-promoted, which is consistent with mZVI particles. However, the high reduction efficiency of nitrate by nZVI particles under neutral condition may be the good reactive activity of nZVI particles, which can not only make the quick reduction of nitrate before the formation of iron oxides, but also react quickly with H_2O to produce H_2, favoring the nitrate reduction.

In summary, the reduction of nitrate by ZVI is often accompanied by the corrosion of ZVI and the variation of H^+ concentration due to the consumption of H^+ by nitrate reduction and the hydrolysis of ferric or ferrous ion. Therefore, the solution pH can severely affect iron corrosion, thus determining nitrate reduction efficiency of ZVI.

2.2.2. Effect of temperature

The change in temperature has a remarkable influence on nitrate reduction. In general, the removal efficiency of nitrate by ZVI increases with the increase of reaction temperature (Ji et al., 2011). At temperatures of 30 °C, the nitrate removal was 67.6% after 10 min, while at temperature of 50 °C, the nitrate removal by nZVI particle was significantly enhanced to 96.2% after 10 min (Hwang et al., 2010). The pseudo first-order rate constants of nitrate reduction by mZVI were 0.36 ± 0.03 and 1.39 ± 0.23 h^{-1} under the unbuffered and buffered conditions at 75 °C, respectively, which exceeded by 5 and 19 times of the rate constant achieved at 20 °C under the unbuffered condition (0.072 ± 0.006 h^{-1}) (Ahn et al., 2008).

Several steps, including nitrate diffusion and adsorption onto iron surface, chemical reaction on the iron surface, and products diffusion into the solution, affect the overall reaction. Increasing reaction temperature will result in an increasing mobility of nitrate molecules to the surface of ZVI particles. In addition, increasing reaction temperature will supply excessive energy to overcome the activation energy barrier. According to the removal efficiency of nitrate at different temperatures, activation energy (*E*a) can be calculated and used to determine the limiting-step of nitrate reduction by ZVI. Diffusion requires less energy than chemical reaction. A typical mass transport-controlled reaction in water is 10–20 kJ/mol. For example, the *E*a for nitrate reduction in batch experiments was reported to be 42.5 kJ/mol for mZVI particles and 25.8 kJ/mol for nZVI particles over the temperature range of 10–60 °C (Liou et al., 2005a). The value of *E*a for mZVI particles is large, suggesting that it is a typical chemical reaction step. Thus, there is a significant degree of reaction control on the kinetics of denitrification in a well-mixed mZVI system. For example, when mZVI with/without pre-treatment by hydrogen gas at 400 °C was used to reduce nitrate, the *E*a calculated by Arrhenius equation was 46.0 and 32.0 kJ/mol for non-pretreated and pretreated iron, respectively, indicating that temperature effect was more significant for non-pretreated iron than that of pretreated iron (Liou et al., 2005b). On the other hand, as the *E*a for nZVI particles is slightly above 10–20 kJ/mol, the kinetics of denitrification is characteristics of mass transport in addition to reaction control. Therefore, the influence degree of temperature on nitrate reduction by mZVI particles is higher than that of nZVI particles.

2.2.3. Effect of DO

Dissolved oxygen (DO) is usually existed in shallow groundwater or wastewater. As a highly active oxidant, DO may exert a crucial effect on iron corrosion and thus on the subsequent removal of nitrate.

There are two contrary potential effects of DO on the nitrate reduction by ZVI. DO may deteriorate the removal rates of nitrate, especially at high DO concentration. For example, the performance of nitrate reduction (100 mg/L) decreased by 40% under aerobic condition by nZVI than that under anoxic condition at the equilibrium state (about 90 min) (Khalil et al., 2016b). Moreover, nZVI reacted more slowly with nitrate in open system than in sealed system, because oxygen in the aqueous solution decreased the reducing capacity of nZVI for nitrate reduction (Wang et al., 2006). 62.3% of nitrate was reduced by nZVI treatment in anaerobic system, but the removal percentage accounted for only 22.1% in aerobic system within 120 min (Zhang et al., 2011). Meanwhile, DO may also enhance nitrate reduction. For instance, the nitrate removal efficiency reached 81% after 3 h in a laboratory continuous-flow ZVI packed bed columns at an initial DO of 8.8 mg/L and initial pH of 8.3–8.5, while it was only 39% at an initial DO of 0.6 mg/L (Westerhoff and James, 2003). The nitrate reduction by ZVI was negligible in the absence of DO at pH > 5; to the contrary, obvious reduction of nitrate was observed in the presence of DO by increasing iron corrosion to produce more ferrous ions. The highest reduction of nitrate occurred at initial pH 2.0, with 49.7% in the presence of DO compared with only 12.1% in the absence of DO (Guo et al., 2015). However, no significant effect of DO on the reaction rates of nitrate was observed (Huang and Zhang, 2005a). Therefore, no general conclusions were obtained about the potential effects of DO on the nitrate reduction by ZVI.

The reasons why the presence of DO will inhibit the nitrate reduction were summarized as follows: (1) DO could compete for electrons; (2) the corrosion products derived from oxygen reduction would interfere the rate of iron dissolution and subsequently the nitrate reduction; (3) the concentration of DO in solution might be related with the formation of various iron corrosion products, which can serve as a physical barrier, a semiconductor or a coordinating surface. For example, in the presence of DO, a two-layer structure with an inner layer of magnetite

and an outer layer of lepidocrocite might be formed, which would deteriorate the performance of ZVI. While as DO being depleted, the outer lepidocrocite layer might be transformed to magnetite, which would not hinder the ZVI performance even in a substantial thickness (Huang and Zhang, 2005a). On the other hand, DO could facilitate the formation of a more reducing condition partially due to the rapid production of dissolved and/or surface-bound Fe(II) by driving very rapid and intensive iron corrosion. Dissolved oxygen (DO) could also accelerate the generation of iron oxides, which can act as adsorption sites.

In our opinion, the role of oxygen in the performance of ZVI may depend on the environmental conditions (such as DO concentration, reaction time, ZVI dosage, solution pH, and so on) and surface properties of materials (such as the number of active site). There are multiple roles of oxygen in the nitrate reduction by ZVI, such as (1) compete the nitrate for reactive sites; (2) facilitate iron corrosion and produce more reducers, such as dissolved and/or surface-bound Fe(II); (3) compete for reducing agents, such as dissolved and/or surface-bound Fe(II) and proton; and (4) accelerate iron corrosion and form more iron oxide passivation layer. The roles of (1), (3) and (4) restrain the nitrate reduction, while the role of (2) enhances the nitrate reduction. These roles can occur independently or in combination, the net effect of DO on nitrate reduction by ZVI will depend on the detail conditions, such as the reaction conditions and the surface properties of materials. Taking DO concentration for example, under the low oxic condition (e.g., below 6 mg/L), the reduction of DO facilitated iron corrosion and produced more aqueous and adsorbed/structural Fe(II), which was beneficial for the removal of nitrate (Yang and Lee, 2005); while under highly oxic conditions, the excess DO would compete for reducing agents, resulting in a decrease of rate constants (Westerhoff and James, 2003). For ZVI dosage, nitrate was completely removed in 2 h when it was 4 g/L under both aerobic and anoxic situations. However, when it was only 1 g/L, 60% of nitrate was reduced in the anoxic system and 40% of nitrate was reduced in the aerobic system in 2 h (Wang et al., 2006). Moreover, at low pH solution, the oxidation of ferrous iron by O_2 is weak and a little iron oxide passivation layer will form, which make DO favor for the nitrate reduction. However, at high pH solution, the DO may play a contrary role for the nitrate reduction. As for the surface properties of materials, the DO usually play a facilitation role for mZVI particles; while an inhibition role for nZVI particles under neutral conditions. Future attempts can be made to find some feasible methods either to minimize the deterioration effects of oxygen or to enhance the ZVI performance.

2.2.4. Effect of groundwater constituents

Groundwater and some wastewater, such as landfill leachate, municipal sewage, etc. typically contain various dissolved anions, such as Cl^-, HCO_3^-, SO_4^{2-}, HPO_4^{2-} and natural organic matters (NOMs), such as humic acid, which may affect the nitrate reduction by ZVI. It is important to consider the influence of these coexisting constituents on the nitrate reduction by ZVI when the ZVI-based permeable reactive barrier (PRB) technology was applied to remediate polluted groundwater with nitrate. Unfortunately, a few works have been carried out for the nitrate reduction. Su and Puls (2004) studied the effects of anions on nitrate reduction, and they found that these anions decreased the nitrate reduction rate in following order: $Cl^- < SO_4^{2-} < PO_4^{3-}$, which was consistent with their affinity to form complexes with iron oxides. The blockage of reactive sites on the surface of ZVI and its corrosion products by specific adsorption of the inner-sphere complex forming ligands (sulfate and phosphate) might be responsible for decreasing nitrate reduction by ZVI relative to the chloride system. In order to discuss the role of these anions, Tang et al. (2012) studied the reductive removal of nitrate by ZVI in the presence of alkaline soil, and they found that the major anions (Cl^-, SO_4^{2-}, and HCO_3^-) could accelerate nitrate reduction due to the promotion of iron corrosion and the possible occurrence of green rusts. However, PO_4^{3-} had inhibitive effect. Compared with the results obtained by Su and Puls (2004), the difference of the influence of ligands on the nitrate removal might be that the reaction medium contained some loess soil.

Humic acid and HCO_3^- are important natural organic matters and inorganic matter, which are widely existed in water, more researches are needed to investigate their influence on the removal of nitrate by ZVI (Ruangchainikom et al., 2006; Shi et al., 2011; Khalil et al., 2018; Wang et al., 2018). Moreover, because of the complexity of the interaction of groundwater constituents with ZVI, more researches are needed to investigate the mechanisms associated with the inhibition of nitrate removal by ZVI in the presence of various anions.

2.2.5. Effect of nitrate concentration

Several previous studies reported that higher initial nitrate concentrations could increase the efficiency of ZVI (Hao et al., 2005a, 2005b). For example, nitrate removal rate increased with the increase of nitrate concentration in a field continuous-flow mZVI packed bed columns (Westerhoff and James, 2003). It was also found that nitrate removal rate increased with increase of nitrate concentration from 20 mg/L to 120 mg/L by nZVI (Liu et al., 2012). The initial nitrate concentration did not significantly influence the final removal efficiency, while the absolute removal of nitrate increased with increasing initial nitrate concentration (Zhang et al., 2010). The reason might be that higher initial nitrate concentration resulted in a larger concentration gradient and the higher reaction probability between iron and nitrate, apparently increasing the removal percentage of nitrate.

The nitrate reduction by ZVI can be described by the first- or pseudo first-order kinetic model, some of results were list in Table 2. It can be seen that the observed reaction rate constant (or half-life) is independent on the initial nitrate concentration within the applied concentration ranges when the reaction is pseudo first-order with respect to nitrate concentration (Zhang et al., 2010; Choe et al., 2000). The reaction rate constant is affected by some factors, such as initial pH, the dosage of ZVI, the physical characteristics of ZVI, temperature, and so on. In general, the lower initial pH, higher dosage of ZVI and higher temperature can lead to higher reaction rate constant. Usually, nZVI particles have higher reaction rate constant than that of mZVI particles. The higher purity of iron surface, the higher reaction rate constant. Table 2 also indicates that there were no comparable results among the ZVI particles because that the difference of reduction condition of nitrate.

According to the published literatures, the first- or pseudo first-order kinetic model was not suitable for the nitrate reduction in an iron-limiting condition or a pH-control or buffer condition. When dosage of nZVI was 2 g/L, the reaction rate constant increased with increase of initial concentration of nitrate (Yang and Lee, 2005). The reduction of nitrate by iron with pH control appeared to be a 1.7 order reaction (Huang et al., 1998). Kim et al. (2016) found that pseudo second-order adsorption kinetic equations were suitable for fitting the nitrate removal in an iron-limiting condition. Xiong et al. (2009) observed that pseudo first-order model was less suitable for describing the chemical reduction of nitrate by nZVI when either nZVI supply was insufficient or when excess amounts of protons were present. Rodríguez-Maroto et al. (2009) found that an Eley–Rideal kinetic model could explain the rate of nitrate reduction at a constant pH value. Huang et al. (2003) proposed a new kinetic model under the acidic pH-control condition and the kinetic constants depended upon pH values. In addition, even if without pH-control, the first- or pseudo first-order kinetic model was not suitable for the nitrate removal due to the specific reaction conditions. For example, Wang et al. (2014) found that both pseudo first-order and pseudo second-order adsorption kinetic equations provided a good fit for the observed nitrate removal without pH-control. The denitrification rate without reaction conditions (DO or reaction pH) control, tended to be a second-order kinetics at pH < 3, and pseudo first-order kinetics at pH > 3 (Fan et al., 2009). Choi et al. (2008) found that lower pH gave the pseudo first-order kinetics, while it was close to the zero-order reaction when the pH of the solution was becoming high and nitrate concentration was higher. Wang et al. (2006) found

Table 2
The reaction rate constant in first- or pseudo first-order kinetic model of nitrate reduction by ZVI.

Size	Specific surface area (m^2/g)	NO_3^- concentration (mg/L)	ZVI dosage (g/L)	Time (h)	Initial pH	Rate constant (h^{-1})	Reference
~50 nm	20–25	131 ± 2	0.5–1.0	40	7.15 ± 0.1	0.002–0.04	(Hosseini et al., 2018)
50 nm,	20–25	105	4	72	Neutral pH	0.012	(Hosseini and Tosco, 2015)
1 ± 100 nm	31.4	50–400	4	–	Natural pH	8.92–9.33	(Choe et al., 2000)
100–200 mesh	–	25	36	–	7.0 with buffer	16.8 ± 1.8	(Siantar et al., 1996)
16.7 nm	46.27	100	1.25	0.25	7	6.30–6.60	(Hwang et al., 2011)
10–20 mesh	1.67	30	12,500	4	6.7	0.072 ± 0.006	(Ahn et al., 2008)
10–20 mesh	1.67	30	12,500	4	7.4 with buffer	0.214 ± 0.015	(Ahn et al., 2008)
10–20 mesh	1.67	30	12,500	4	6.7 (75 °C),	0.36 ± 0.03	(Ahn et al., 2008)
40 mesh	~2.30	16.5	50	–	7.0 with buffer	0.049 ± 0.04	(Alowitz and Scherer, 2002)
<100 mesh	0.516	177	7.7	0.33	6.5–7.5 with buffer	0.486	(Liou et al., 2005b)
160–200 mesh	0.06	50–400	4	2	2	2.0–2.17	(Fan et al., 2009)
325 mesh	–	15	80	–	5.0–7.0	3.18–0.86	(Cheng et al., 1997)
1–20 nm	25.4	20	0.5	2	4–7 with buffer	0.37–0.2	(Chen et al., 2004)
90 nm,	49.46	100	2.88	2	5.86–6.70	2.4	(Ghosh et al., 2017)
20 nm	65.74	100	2.88	2	5.86–6.70	0.66	(Ghosh et al., 2017)
<100 nm	8.1	50	0.57–2.86	–	~7	2.26–10.12	(Sohn et al., 2006)
20–70 nm	16.67	177	0.35	–	6.8	0.8	(Liou et al., 2005a, 2005b)
16.7 nm	79.06	100	1.25	–	7, 30 °C	4.08	(Hwang et al., 2010)
1–100 nm	12.4	50	1.0	–	6.7	5.16	(Zhang et al., 2010)

that the n^{th}-order reaction model was suitable to describe chemical reduction of nitrate by nZVI at a rather high intensity of mixing and without pH-control, and the reaction order was from 0.26 to 0.66, and k_{obs} was from 1.08 to 0.44 mg-N L^{-1} ln min^{-1} when the initial concentration of nitrate was 30 mg/L to 80 mg/L. Huang and Zhang (2002) developed a kinetic model with a double-Langmuir-adsorption model to represent site saturation effects of aqueous Fe^{2+} and NO_3^- on nitrate reduction in a ZVI system at near neutral pH value.

It can be seen that above-discussed operational parameters can affect nitrate reduction by ZVI. Thus, the removal efficiency of nitrate may increase by the optimization of operational parameters, such as decreasing solution pH, increasing reaction temperature, controlling the concentration of DO or nitrate, or decreasing the concentration of interfering ion, and so on. It may be a most efficient strategy to reduce nitrate at acidic condition. However, the nitrate reduction in acidic aqueous solution would lead to inconvenient operation and the consumption of acid or alkali agent. Therefore, more and more interests focused on the near-neutral or neutral conditions. Prone to agglomeration and poor stability, nZVI particles alone could decrease its reduction capacity although some nZVI particles alone can reduce nitrate in neutral conditions. Therefore, the improvement of the chemical composition and structure of ZVI composite, as well as the addition of reduction assistants such as metal ion, light, complexant or hydrogen, are two mostly used strategies to overcome the above-mentioned disadvantages of ZVI. In addition, because the end product of nitrate reduction by ZVI particles alone was mainly ammonia, which makes investigators seek solutions for increasing the N_2 selectivity.

3. Strategies for improving the efficiency and N_2 selectivity of nitrate reduction

3.1. Optimization of chemical composition and structure of ZVI composites

The chemical composition and structure of ZVI composites have important influence on the adsorption capacity to nitrate and the active site for transferring electron to nitrate, as well as on the distribution of iron oxides on the surface of ZVI composites during the process of nitrate reduction.

3.1.1. Doped ZVI composites

The doped ZVI composites usually consist of ZVI and some high electrode potential metal (such as Cu^0) or carbon. In doped ZVI composites, ZVI and the high electrode potential material can form macroscopic galvanic cells, which enhance nitrate reduction even in near-neutral aqueous solutions in comparison with ZVI particles alone. For example, batch tests of nitrate reduction by ZVI-AC and ZVI at initial pH 2–6 were carried out within 720 min, and the results showed that with increasing initial pH, two systems performed discriminately in nitrate reduction. However, the efficiency of nitrate reduction by ZVI-AC remained 73% even at initial pH 6, whereas that by ZVI only dropped drastically to around 10% (Luo et al., 2014). It was also found that reduction efficiency of nitrate by tri-metal 10% (Pd—Cu)–nZVI was higher than bare nZVI, and the catalyst Cu and Pd helped enhance higher efficiency of nitrate removal (Lubphoo et al., 2015). More than 80% nitrate was reduced by nZVI-5% Cu particles (w/w) within 20 min, and complete removal was attained within 1 h; while 74.5% nitrate was removed by uncoated nZVI within 1 h (Sparis et al., 2013). The nitrate reductive activity by Pd-ZVI was 2.72%, which was 1.85 times higher than that of hybrid without Pd (Jiang et al., 2015). Moreover, the nitrate reductive activity of doped ZVI composites was also studied through packed sand column test. The best condition to remove nitrate among nZVI/sand columns was obtained when a single 10-cm high layer of nZVI/sand was used, and >97% influent nitrate was removed; while in (Cu-nZVI)/sand columns, the optimum performance was reached when double 5-cm high layers of (Cu-nZVI)/sand was used, and a complete removal of nitrate was attained. Furthermore, Cu-nZVI particles showed better removal efficiency than nZVI for nitrate reduction in the simulated groundwater (Shubair et al., 2018). It was also found that the recorded values of reduced nitrate by bare nZVI and 2.5% Cu-nZVI were similar during the reaction time, but at the end of reaction (after 200 min), 2.5% Cu-nZVI was more efficient than bare nZVI for nitrate reduction (Hosseini et al., 2011).

The reduction activity for nitrate by doped ZVI composites was summarized in Table 3. The nitrate reduction was enhanced by doped ZVI composites, which was mainly attributed to: (1) a relative potential difference in galvanic cells drives much more electrons from ZVI to second substance during micro-electrolysis process rather than iron corrosion only; (2) the nitrate reduction was mainly performed on the surface of the doped substance, which decreased the competition between nitrate and iron oxide for the active sites of surface; (3) H^+ can be generated by the hydrolysis and oxidation of high concentration of ferrous ions from the high corrosion rate of iron or by the quick reduction of H_2O on the surface of the doped substance, which makes it possible for nitrate to be reduced at near-neural pH value.

In doped ZVI composites, the type and content of doped metal have influence on the activity of doped ZVI composites for nitrate reduction. The nitrate reduction by 5.0% (w/w) bimetal particles (nano-Pd/ZVI, nano-Pt/ZVI and nano-Cu/ZVI) under the Ar-purged buffered solution

Table 3
The reduction activity for nitrate by doped ZVI composites.

ZVI composite	NO_3^- concentration (mg/L)	Composite dosage (g/L)	Time (h)	Reduction at near-neural pH	Reduction products	Reduction by ZVI	Reference
ZVI-AC	221	50		73%	~100% NH_4^+	~10%	(Luo et al., 2014)
ZVI-0.06% Pd	886	–	7	75%	30% N_2, ~70% NH_4^+	–	(Choi et al., 2008)
nZVI–10% (Pd—Cu)	100	0.25 g	1	90%	~60% N_2, ~40% NH_4^+	~50%	(Lubphoo et al., 2015)
nZVI-5.0% Cu	~177	0.35	1	~100	80–60% NH_4^+, 20–40% NO_2^-	52%	(Liou et al., 2005a, 2005b)
nZVI–2.35% Ag	531.6	3	4	27.25	–	18.85%	(Singh et al., 2012)
nZVI-1 wt% Au	~200	1.5	1.5	~77%	~6% NO_2^-, 50% NH_4^+	~42%	(Su et al., 2014)
ZVI-0.3 wt% Pd-0.5 wt % Cu	177	7.7	6	~91.5%	30% N_2, 24.0% NH_4^+, 2.0% NO_2^-	–	(Liou et al., 2009)
nZVI-5% Cu	200	3.3	1	~100%	74% NH_4^+	74.5%	(Sparis et al., 2013)
nZVI-0.01% Ni	20	2	1	~90%	93.55% NH_4^+, 0.33% NO_2^-	~80%	(P. Li et al., 2017; X. Li et al., 2017)
ZVI-5% Cu	57.25	0.86	1	~100%	87% NH_4^+	~80%	(Muradova et al., 2016)

in 75 mL was compared. The results showed that the deposited metals were ranked Cu > Pd > Pt in their promotion on nZVI reactivity towards nitrate (Liou et al., 2009). The influence of doped metal content on reactivity of the bimetallic ZVI composites for nitrate reduction was investigated, and the optimal loading ratio was found to be <10% (w/w) (Lubphoo et al., 2016). For example, the optimal loading in Cu-ZVI composites was usually 5% (Liou et al., 2009; Sparis et al., 2013; Guo et al., 2018; Shubair et al., 2018).

In doped ZVI composites, the doped metal will affect the product of nitrate reduction. Though ammonia was found to be the predominant end product in nZVI and Cu/nZVI systems, as for nitrite, 40% of the reduced nitrate remained in Cu/nZVI system (Liou et al., 2009). The addition of Pd improved the gas production in nitrate reduction from the recovery rate of nitrate, nitrite and ammonium both in aqueous solution and support solid phase (Jiang et al., 2015). However, nano-composite of tri-metals, (Pd—Cu)–nZVI, could enhance N_2 gas selectivity. Lubphoo et al. (2016) found that N_2 selectivity was 60.5% by the trimetal (Pd—Cu)–nZVI 10% (Pd—Cu) loading with ratio of 2:1 (Pd:Cu). An optimum N_2 of ~30% was obtained in the alkaline solution by 0.3 wt% Pd-0.5 wt% Cu/ZVI, suggesting that the ZVI deposited Pd and Cu could promote the abstraction of oxygen from NO*x* by adsorbed atomic hydrogen on the Cu surface, and enhance nitrogen gas formation on the Pd surface (Liou et al., 2009). Even so, the N_2 selectivity was still low by doped ZVI composites.

3.1.2. Supported ZVI composites

To overcome the drawbacks of nZVI particles alone, such as agglomeration (Ryu et al., 2011), which can significantly decrease the effective surface area of nanoparticles, and thus reduce their catalytic performance, the supported ZVI composites have been developed.

Many supporting materials were used, including organic materials, such as alginate substrate (Lee et al., 2016; Cho et al., 2015), polymerstyrene anion exchanger (Jiang et al., 2012), polystyrene resins (Jiang et al., 2011), chelating resin (Shi et al., 2013), organic polymeric beads (Jiang et al., 2015); inorganic materials, such as carbon materials (nano-graphenes (Salam et al., 2015), exfoliated graphite (Zhang et al., 2006), activated carbon (Khalil et al., 2016a, 2016b; Khalil et al., 2018), biochar (P. Li et al., 2017; X. Li et al., 2017)), clay minerals (pillared clay (Zhang et al., 2011), palygorskite (Frost et al., 2010; Xi et al., 2014; Dong et al., 2018), diatomite (Sun et al., 2013; Ma et al., 2016; Hao and Zhang, 2017), bentonite (Li et al., 2009; Xi et al., 2011; Zhao et al., 2018), kaolin (Cai et al., 2014; Shi et al., 2014)), zeolite (NaY zeolite (Zeng et al., 2017), clinoptilolite (Fateminia and Falamaki, 2013)), γ-aluminum oxide (Hao and Zhang, 2017), silicon (Anbia and Kamel, 2018) and biotite (Cho et al., 2010). These support materials can be used to immobilize nZVI without decreasing its reactivity. The most frequently used methods for synthesizing these supported ZVI composites include coating the surface of nZVI, emulsification of nZVI, deposition of nZVI on a carrier, or trapping nZVI in a matrix. The supported ZVI composites have often higher surface area than that of unsupported ZVI. The physical-chemical properties of support matrix play an important role in the particle size and distribution of the incorporated nZVI (Jiang et al., 2012).

The supported ZVI composites have one or more of the advantages in the catalytic performance, such as (1) higher reduction efficiency of nitrate than that of nZVI; (2) higher reduction efficiency of nitrate at neutral pH condition. The reduction efficiency of nitrate by supported ZVI composites was often 0.5–2 times higher than that of nZVI at the same reduction condition (Jiang et al., 2015; Lee et al., 2016; P. Li et al., 2017; X. Li et al., 2017; Zhang et al., 2011), because support matrix can not only prevent the agglomeration of nZVI, which provides a larger accessible surface area, but also serve to pre-concentrate reactants by adsorption, which promotes the mass transfer of nitrate from solution onto iron. Moreover, support matrix also serves to mediate electron transfer reactions, and nucleate the growth of product phases. The nitrate reduction by supported ZVI composites is an acid-driving process. However, high removal of nitrate by many supported ZVI composites can also be achieved at neutral pH (Dong et al., 2018; Shi et al., 2016; Shi et al., 2013), because many support matrix have mesoporous structure, the active sites within the inner pore structure can reduce nitrate even though the metal hydroxide is present mainly on outer surface. Another reason is that the functional groups of the carboxyl (–COOH/–COO^-) groups on supporting matrices can react with H^+ or OH^-, hence offsetting the impact of pH changes. In addition, the influence degree of pH on the reduction efficiency of nitrate is also determined by acid or base site of supporter. Some support matrix can act as the proton-donor, which also improves the removal efficiency of nitrate at neutral pH value.

Supported ZVI composites can help decreasing the total nitrogen amount in water, which was proved by the following aspects: (1) ammonia is the end product of nitrate reduction by ZVI alone, while supported ZVI composites can reduce the selectivity of ammonia in the product of nitrate reduction. For example, ammonia is the main end-product of nitrate reduction by supported ZVI composites, and the N_2 yields of product of nitrate reduction by supported ZVI monometallic composites remain below 10% (Zhang et al., 2006). However, the N_2 selectivity was about 70% by supported ZVI bimetallic composites, such as Fe/Pd composite (Shi et al., 2016); (2) moreover, some support matrix can adsorb ammonia and release into aqueous solution under neutral pH (Fateminia and Falamaki, 2013).

The catalyst and the physical-chemical properties of the carriers are main factors that significantly influence the catalytic performance of supported ZVI composites. It is confirmed that bimetallic catalysts are more efficient than monometallic catalysts and the active ingredients comprising of a noble metal usually have good catalytic activity (Hao and Zhang, 2017).The physical-chemical nature of the carrier (such as

surface state, constituent, chemical stability, etc.) has influence on the reaction process, because (1) the carrier's surface area is related to the high dispersal of the active metallic ingredients and the adsorption of nitrate and its reduction product (Zhang et al., 2006; Lee et al., 2016; Khalil et al., 2016a); (2) the carrier's pore structure and surface charge are related to the mass transfer of nitrate and its reduction product from solution to iron surface (Shi et al., 2013, 2016); (3) the carrier's surface functional groups or ions are related to the immobilization of ZVI and the reduction products of nitrate, such as ammonia (Salam et al., 2015). The surface functional groups of carrier play a significant role in the particle size, distribution and reactivity of the incorporated nZVI. In general, the positively charged ammonium group is more favorable than the neutral chloromethyl group to form smaller nZVI particles, thereby enhances their reactivity for nitrate reduction (Jiang et al., 2011). Moreover, the immobilization of ammonia can be achieved by the ion exchange reaction of surface ion.

There are many limitations, which affect the reduction performance of supported ZVI composites. For example, the low attachment of nZVI on the substrate surface (<10 wt%) and uneven distribution of nZVI on the supporting materials (Lee et al., 2016); and the highly dispersed nZVI in supported ZVI composites, which can be easily oxidized to iron oxides, and decrease their reduction ability. Moreover, the relationship between the characteristics of the loaded nZVI and their performance needs further investigation (Jiang et al., 2012).

The reduction activity for nitrate by supported ZVI composites is listed in Table 4.

3.1.3. Premagnetized ZVI

Premagnetization has been used to enhance the reactivity of ZVI based on the good magnetic memory (remanence) function of ZVI (P. Li et al., 2017; X. Li et al., 2017). ZVI or ZVI composites are firstly premagnetized in a desired magnetic field (Zaidi et al., 2013). When the external field is removed, the premagnetized ZVI or ZVI composites still remains magnetized (Ghosh et al., 2012). During the nitrate reduction process, an inhomogeneous magnetic field around the premagnetized ZVI or ZVI composites particles will generated, which can not only facilitate the transportation of NO_3^- and Fe^{2+}, but also accelerate the corrosion of iron by enhancing the mass transfer (Fe^{2+}, H^+, etc.), favoring the reduction of nitrate. Furthermore, the Lorentz force can also promote the mass transfer process (Li et al., 2019), and hence enhance the reaction rate. It was found that the nitrate reduction rates of premagnetization Fe^0/(Fe/Cu) system was 2.17 times higher than that of un-premagnetization Fe^0/(Fe/Cu) system. Similarly, the nitrate reduction rate of premagnetization Fe^0 system was 1.99 times higher than that of Fe^0 system (Ren et al., 2017).

During the reduction of nitrate by premagnetized ZVI or ZVI composites particles, the nitrate can be concentrated on the surface of particles of premagnetized ZVI or ZVI composites by the intensity of magnetic field gradient force. Since the higher concentration of nitrate is beneficial to select the nitrogen and can provide more opportunities for N—N recombination (for nitrogen generation). Therefore, the premagnetized ZVI or ZVI composites can also enhance the N_2 selectively of nitrate reduction. The selectivity efficiency for nitrate reduction ([TN removal]/[NO_3^--N removal] ratio) by premagnetization Fe^0/(Fe/Cu)system and premagnetization Fe^0 system were 54.3% and 40.0%, respectively, while 38.2% of that by Fe^0/(Fe/Cu) system, and 30.1% of that by Fe^0 system, respectively (Ren et al., 2017).

3.2. Addition of reducing assistants

3.2.1. Metal cations

The addition of metal cations also affects the nitrate reduction. Fe^{2+}, Fe^{3+}, Al^{3+} and Cu^{2+} ions were often added into the reduction systems of nitrate by ZVI (Han et al., 2016; Huang et al., 2003; Huang and Zhang, 2005b, 2006; Khalil et al., 2016b; Tang et al., 2012; Xu et al., 2012). Fe^{2+} can reduce nitrate in theory, but the removal of nitrate under initial acid conditions is low. For example, around 10% of the removal efficiency of nitrate (50 mg/L) under initial neutral conditions by Fe^{2+} (50 mg/L) alone were observed (Han et al., 2016). When Fe^{2+} was added in the Fe^0/nitrate system under initial neutral conditions, the nitrate reduction rate and removal efficiency was significantly improved. Especially, the iron oxides (e.g. Fe_3O_4, FeOH(OH), α-FeO(OH))

Table 4
The reduction activity for nitrate by supported ZVI composites.

ZVI composite	NO_3^- concentration (mg/L)	Composite dosage (g/L)	Time (h)	Reduction results		Compared with unsupported ZVI composites		Reference
				Reduction at near-neural pH	Reduction production	Reduction at near-neural pH	Reduction products	
nZVI/alginate substrate	90	–	2.0	73%	–	73%	–	(Krajangpan et al., 2008)
nZVI/nanographenes	50	3	24	74.7%	68% undetectable nitrogen species, 3.0% NH_4^+	59.8%	45% undetectable nitrogen species, 20% NH_4^+	(Salam et al., 2015)
nZVI/pillared clay	500	0.5	2	100%	Main NH_4^+	62.3%,	Main NH_4^+, small NO_2^-	(Zhang et al., 2011)
nZVI/exfoliated graphite	80	1.67	0.5	100%	87% NH_4^+, <4% NO_2^-	~40%		(Zhang et al., 2006)
nZVI/NaY zeolite	100	6	6	100%	80% N_2, 20% NH_4^+	68.0%	NH_4^+ 99.0%	(Zeng et al., 2017)
nZVI-Cu/NaY zeolite	100	6	6	100%	85% N_2, 15% NH_4^+	~90%	70% N_2, 30% NH_4^+	(Zeng et al., 2017)
nZVI/attapulgite	20	2.0		~83.8%	72.1% NH_4^+	15.3%	14.1% NH_4^+	(Dong et al., 2018)
nZVI/AC	200	1	1.5	54%	~27.2% NH_4^+, ~5.5% NO_2^-, ~5.5% N_2	41%	~9.2% NO_2^-, ~13.9% N_2	(Khalil et al., 2016a, 2016b)
nZVI/pillared bentonite	100	–	100	100%	~93% NH_4^+, a little NO_2^-, little N_2	30%, initial pH of 3	–	(Li et al., 2009)
nZVI/SiO_2–FeOOH	64	4	–	67.18%	–	–	–	(Ensie and Samad, 2014)
nZVI-Ni/biochar	20	2	1	~100%	98% NH_4^+, 0.1% NO_2^-	90%	93.5% NH_4^+, 0.3% NO_2^-	(P. Li et al., 2017; X. Li et al., 2017)
nZVI-Ni/kaolin	40	2.5	0.5	26.9%	–	–	–	(Cai et al., 2014)
nZVI–Pd/chelating resin	88.5	160 mg Fe/L	5	100%	69.2% N_2	–	–	(Shi et al., 2016)
ZVI-Pd/D201 anionic exchanger	221	2.4	8.3	50%	>97% NH_4^+	–	–	(Jiang et al., 2015)
ZVI-Cu/zeolite	30	60	30	~60%	Main NH_4^+, <1% NO_2^-	–	–	(Fateminia and Falamaki, 2013)

would be formed and the Fe(II) adsorbed on these iron oxides could further facilitate the reductive efficiency of nitrate (Han et al., 2016; Williams and Scherer, 2004; Xu et al., 2012). A reasonable explanation for the improvement of Fe^{2+} for the reductive efficiency of nitrate may be that, Fe(II) on the surface of iron with a stronger reducing property than Fe^{2+} in the solution, as well as the H^+ consumption of the nitrate reduction of the system can be supplied by the hydrolysis of Fe^{2+}. Han et al. (2016) revealed that Fe^{2+}_{aq} and the characteristics of minerals on the surface of ZVI played an important role in nitrate reduction. Both nitrate reduction and the decrease of Fe^{2+}_{aq} exhibited similar kinetics and were mutually promoted, depending upon the types of the surface iron oxides of ZVI. Additionally, further reduction of nitrate produced more surface iron oxides, supplying more active sites for Fe^{2+}_{aq}, resulting in more electron transfer between Fe^{2+} and surface iron oxides, and a higher reaction rate (Suzuki et al., 2012). The addition of Fe^{3+} also improved the nitrate reduction rate by ZVI, which might be attributed to the increased Fe^{2+} availability (according to Eq: $Fe^0 + 2Fe^{3+} \rightarrow 3Fe^{2+}$) (Tang et al., 2012).

The presence of Cu^{2+} increased removal efficiency and kinetics around 3.5 times more than that by ordinary pristine nZVI alone, i.e., nitrate reduction time was reduced from 1 h to 20 min (Khalil et al., 2016b). The reason for high kinetic rate and better performance is attributed to: (1) the presence of Cu^{2+} stimulated the corrosion of iron in higher amounts and faster rates, yielding more electrons for nitrate reduction, increasing initial ferrous and protons concentration in the reaction medium, which favors nitrate reduction; (2) copper and its compounds can act as an inert electrode or provide catalytic surface on which indirect electron transfer can reduce proton to form hydrogen, which is a more powerful reducing specie than electron transfer (Hao et al., 2005a, 2005b; Ren et al., 2016). It was also found that cation significantly enhanced nitrate reduction with an order of $Fe^{3+} > Fe^{2+} > Cu^{2+}$, through providing Fe^{2+}directly or indirectly (Tang et al., 2012).

3.2.2. Ligand

The ligand effects on nitrate reduction by ZVI are summarized from three aspects: (1) the ability to offer potentially dissociable protons from the ligands (Song et al., 2017); (2) the complexation ability to dissolve the passive oxide layer on the surface of iron, as well as their buffer performance (Singh et al., 2012); and (3) the ability to lower the redox potentials of iron species. Therefore, the addition of ligand can promote the nitrate reduction rate by ZVI at near neutral condition. Song et al. (2017) found that at an initial nitrate concentration of 20 mg N/L, the pseudo first-order reduction rate constant of nitrate in the ZVI-acetylacetone (AA)-NO_3^- system was 0.0991 h^{-1}, which was 52 times higher than that in the ZVI-NO_3^- system. Under otherwise identical conditions, the other five ligands, including EDTA, formate, acetate, oxalate, and phosphate, had negligible effects on nitrate reduction. In this strategy, it is important to choose the suitable ligands. For instance, EDTA significantly enhanced nitrate reduction by zero-valent bimetallic (Fe—Ag) nanoparticle, via adsorption and complexation with the iron corrosion products (Singh et al., 2012). However, some inner-sphere complex of iron formed by specific adsorption could block up reactive sites on the surface of ZVI, and decreased nitrate reduction by ZVI. For example, Su and Puls (2004) found that nitrate reduction rates (pseudo-first order) decreased in the following order: citric acid < oxalic acid < formic acid < HCl, ranging from 0.00278 to 0.0913 h^{-1}. Correlation analysis showed a negative linear relationship between the nitrate reduction rates for the ligands and the conditional stability constants for the soluble complexes of the ligands with Fe^{2+} ($R^2 = 0.701$) or Fe^{3+} ($R^2 = 0.918$) ions.

3.2.3. Hydrogen gas

Hydrogen gas could act as a reducing agent to prevent the formation of iron oxide layer through nZVI corrosion due to DO (Lin et al., 2003). Therefore, H_2 could accelerate the kinetic reaction rate of nitrate by nZVI. However, H_2 supply did not significantly increase nitrate removal in the presence of nZVI alone, due to a lack of adsorption of H_2 to Fe sites (Hamid et al., 2015). Pd/nZVI composite could increase the adsorption of H_2 to Pd sites. However, limited improvement of nitrate removal by Pd/nZVI was obtained, because H_2 adsorbed on Pd sites could not reduce nitrate. It was proved that the H_2 adsorbed on Cu sites could accelerate the reduction of nitrate to nitrite, and the H_2 adsorbed on Pd sites could promote the further reduction of nitrite to ammonia or nitrogen gas (Hamid et al., 2015). Therefore, Cu–Pd/nZVI composite combined with H_2 was used for the nitrate reduction (Hamid et al., 2015). Lubphoo et al. (2015) found that the nitrate removal by Cu–Pd/nZVI catalyst in the presence of H_2 was 20% higher than that without H_2.

During the nitrate reduction by Cu–Pd/nZVI, the feeding H_2 gas was not only directly bound onto Cu surface to accelerate nitrate reduction, but also bound onto Pd surface to reduce nitrite to N_2 or undesired ammonia. Moreover, the feeding H_2 gas provided synergistic effect to suppress ammonia formation. For example, Lubphoo et al. (2016) found that in the absence of H_2 feeding into the reaction, the selectivity (N_2/NH_4^+) of (Pd—Cu)–nZVI was 38:56, while it increased to 51:42 in the presence of H_2. Hamid et al. (2015) studied the catalytic nitrate removal in a continuous reactor system using Cu–Pd/nZVI, and found that Cu, Pd, and a proper supply of H_2 were essential for enhancing the removal efficiency and N_2 selectivity, and a complete nitrate removal was finally achieved at 9 h, with 48% nitrogen gas selectivity. The catalytic hydrogenation of nitrate in water has been carried out over Fe/C catalysts at ambient temperature using batch and continuous reactors. It was found that nitrate reduction activity was 2.9 mmol·g $metal^{-1}$ min^{-1}, with nearly 100% selectivity towards nitrogen (Shukla et al., 2009).

3.2.4. Light

ZVI was always loaded on the semiconductor photo-catalysts, such as TiO_2 to increase the promoting effect of light for nitrate reduction (Kobwittaya and Sirivithayapakorn, 2014; Pan et al., 2012; Tugaoen et al., 2017). There was no certain conclusion whether the addition of TiO_2 would improve the removal of nitrate under UV irradiation. For example, Krasae and Wantala (2016) found that the activity of Cu–nZVI/TiO_2 for nitrate removal was better than that without TiO_2. However, Pan et al. (2012) observed that both nZVI and TiO_2/nZVI could effectively remove nitrate. The reason might be that the solution pH was not controlled during the reaction for the former; while acetate was used as buffer to control pH during the reaction for the latter.

Even so, the N_2 selectivity of Cu-nZVI/TiO_2 and nZVI/TiO_2 was higher than that without TiO_2 under UV irradiation. For instance, in nZVI system, the majority of nitrate was converted to ammonia, while only 10% was transformed to N_2. In contrast, around 40% of nitrate was converted to N_2 inTiO_2/nZVI system (Pan et al., 2012). Liu et al. (2014) prepared TiO_2/ZVI by chemical vapor hydrolysis deposition and used it as photo-catalyst, while HCOOH was used as a hole scavenger for nitrate reduction, and they found that the N_2 selectivity was up to 60.9%. The N_2 selectivity was 82% for Cu–nZVI/TiO_2 with 75 mg/L initial nitrate concentration in neutral solution, while it was about 78% for Cu–nZVI at the same condition.

The roles of loading TiO_2 particles and UV irradiation for enhancing denitrification performance of ZVI are possibly as follows (1) the oxidation of ZVI to higher oxidation species is prevented, which maintains a high concentration of ferrous ion, which is critical in nitrate conversion and also delays the formation of the surface oxide layers on nZVI simultaneously (Hsieh et al., 2010; Pan et al., 2012); (2) with the help of TiO_2 catalyst, large amount of H_2 are released to further promote the reduction of nitrate (Lucchetti et al., 2017); and (3) allowing photo-generated electrons to contribute to the nitrate reduction and also to the recovery of nZVI via reduction of oxidized iron species (Sá et al., 2009). Although nZVI/TiO_2 or Cu–nZVI/TiO_2 composites exhibited better performance than nZVI alone under UV irradiation, the selectivity towards N_2-gas, which was 38–80%, was still considerably inferior to the selectivity by other photo-catalysts. Many researchers reported that photo-generated reducing species (e.g., $CO_2^{\bullet -}$) radicals formed from some

scavengers, such as methanol, oxalic acid, and formic acid, etc., could increase the N_2 selectivity in the photocatalytic reduction of nitrate (Doudrick et al., 2013; Shaban et al., 2016; Tugaoen et al., 2017; Zhang et al., 2005). However, relatively a little information is available on the role of $CO_2^{\bullet-}$ in the nitrate reduction by the photocatalytic system using nZVI composite as catalyst.

4. Mechanism and pathway of nitrate reduction

4.1. ZVI alone

When ZVI is added to the aqueous solution, the protons and nitrate are adsorbed onto the surface of ZVI and electrons are released from ZVI for nitrate reduction. The adsorbed protons are also converted into adsorbed atomic hydrogen (H_{ads}) by accepting electrons. Nitrate can also be reduced by H_{ads} (Ahn et al., 2001; Suzuki et al., 2012). The nitrate reduction by ZVI alone is carried out according to following reactions (Eqs. (1)–(8)) (Chen et al., 2005; Cheng et al., 1997; Rodríguez-Maroto et al., 2009):

$$Fe^0 \rightarrow Fe^{2+} + 2e^- \quad (1)$$

$$5Fe^0 + 2NO_3^- + 12H^+ \rightarrow 5Fe^{2+} + N_2 + 6H_2O \quad (2)$$

$$4Fe^0 + 2NO_3^- + 10H^+ \rightarrow 4Fe^{2+} + NH_4^+ + 3H_2O \quad (3)$$

$$Fe^0 + 2NO_3^- + 4H^+ \rightarrow Fe^{2+} + 2NO_2^- + 2H_2O \quad (4)$$

$$6Fe^{2+} + NO_2^- + 8H^+ \rightarrow 6Fe^{3+} + NH_4^+ + 2H_2O \quad (5)$$

$$\text{At acidic condition}: Fe^0 + 2H^+ \rightarrow Fe^{2+} + H_2 \quad (6)$$

$$\text{At neutral condition}: Fe^{2+} + Fe^{3+} + H_2O \rightarrow \text{iron oxides} + H^+ \quad (7)$$

$$Fe^0 + 2H_2O \rightarrow \text{iron oxides} + H^+ \quad (8)$$

Then, the reduced form of nitrogen is desorbed from ZVI surface into the solution. After ZVI transfer electron, ferrous ion is formed. The OH^- concentration increases gradually due to the consumption of protons. The ferrous ion can be oxidized by nitrite or DO at high pH solution. Under such conditions, the primary oxidized products were in the form of various iron oxides (Fe_2O_3, Fe_3O_4, a-FeOOH, b-FeOOH, c-FeOOH, etc.) (Huang et al., 2003; Sohn et al., 2006), which decreased the rate of electron transfer. The components of iron oxides depended on the size of ZVI, the morphology of ZVI, pH of the solution, DO in solution, reduction time etc. (Huang and Zhang, 2005a). It was found that black coating, consisting of Fe_2O_3, Fe_3O_4 and FeO(OH), was formed on the surface of iron grains as an iron corrosion product when the system initial pH was lower than 5 and without dissolved oxygen control. The proportion of FeO(OH) increased as reaction time went on, whereas the proportion of Fe_3O_4 decreased (Fan et al., 2009). Kim et al. (2012) found that the air-stable shell layers of Fe^{BH} nanoparticles consisted of amorphous magnetite and maghemite, and those of Fe^{H2} nanoparticles had only magnetite. The shell layer of Fe^{BH} nanoparticles remained unchanged during aging, while the shell layer of Fe^{H2} nanoparticles increased during aging.

During nitrate reduction process, many influencing factors determined the efficiency of nitrate reduction, such as the mass transfer rate of nitrate from solution onto iron particle surface and the reduction products from iron surface into solution, and the chemical reaction rate of nitrate on the iron particle surface. Higher initial nitrate concentration, higher solution temperature and higher surface area of iron particles, all will benefit the reduction efficiency of nitrate due to the increase of transfer rate of nitrate onto iron surface. High reduction efficiency can also be obtained by the adsorption removal of ammonia formed on iron surface by zeolite (Zeng et al., 2017), owing to the increase of mass transfer of reduction products. Chemical reaction rate of nitrate on the iron surface was affected by the surface electron concentration and activation energy. The reduction efficiency of nitrate decreased on the surface of iron with passivation layer, because the surface passivation layer inhibited the transfer of electron from iron to nitrate. The reduction efficiency of nitrate by nZVI was higher than that by mZVI, it was also higher by pretreated mZVI using H_2 than that by mZVI (Liou et al., 2005b), partially due to the lower activation energy of nZVI or pretreated mZVI using H_2.

Nitrate reduction by ZVI alone includes two steps: $NO_3^- \rightarrow NO_2^- \rightarrow NH_4^+$ or N_2 (Huang and Zhang, 2006), and the main product of nitrate reduction is ammonia. The nitrate or nitrite can gain electrons on the surface of ZVI and then be reduced (Fig. 3). Moreover, Fe^{2+} in acid solution or on the surface of ZVI particles are confirmed as powerful reducing agents for nitrite reduction (Xu et al., 2012; Yang et al., 2018; Zhang et al., 2019), suggesting that nitrate was firstly converted into nitrite on the surface of ZVI, then the formed nitrite was further reduced to ammonia in acidic solution or on the surface of ZVI in neutral solution.

4.2. Mechanism of enhancing the nitrate reduction efficiency by ZVI

According to basic processes of the nitrate reduction by ZVI alone, it can be concluded that two conditions at least must be satisfied for keeping the nitrate reduction by ZVI at a sustainable rate: (1) supplying adequate protons to favor the nitrate reduction; (2) minimizing as much as possible the adverse effect of iron oxides. Therefore, it may be feasible for enhancing the nitrate reduction efficiency by ZVI: (1) accelerating the corrosion rate of iron in order to increase the abilities of offering electron; (2) increasing the concentration of ferrous ions or the surface associated Fe(II); and (3) adding non-ferrous reducing assistants to provide synergistic effects with ZVI.

4.2.1. At acidic condition

It has mentioned above that the nitrate reduction in acidic solution by ZVI can reach high efficiency (Huang and Zhang, 2004). A lot of protons favor not only for the nitrate reduction, but also for the inhibition of the formation of iron oxides. Moreover, many ferrous ions are generated through the reduction of protons by ZVI, which helped the reduction of nitrate.

4.2.2. At neutral condition

In neutral condition, the protons can be supplied through following ways: (1) the reaction of ZVI and H_2O (Dong et al., 2018), as shown in Eq. (8). The nZVI has higher activity to reduce H_2O for the generation of protons than that of mZVI, which is one of the reasons that nZVI

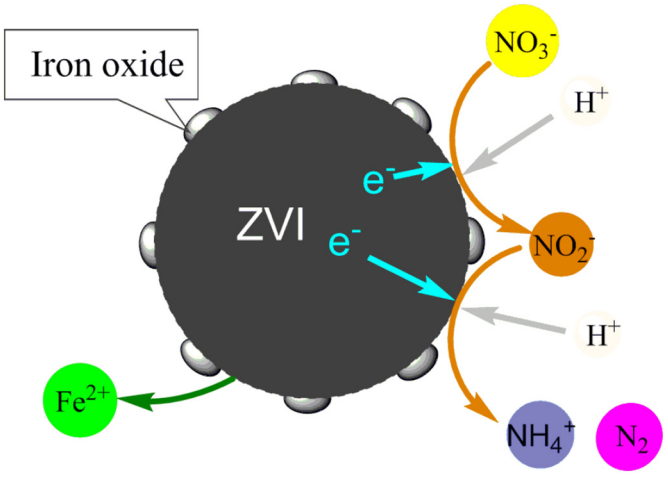

Fig. 3. Schematic representation of nitrate reduction by ZVI.

has higher efficiency for nitrate reduction; (2) the oxidation and hydrolysis of ferrous ions (Yang et al., 2018), as shown in Eq. (7); and (3) the addition or generation of hydrogen donor, such as some of the carriers supported ZVI composites (Cho et al., 2015; Lee et al., 2016; Zhao et al., 2018), the addition of H_2 (Lubphoo et al., 2015) and the generation of H_2 by the photocatalytic water splitting process (Krasae and Wantala, 2016).

In neutral condition, a series of pathway can lessen the adverse effect of iron oxides: (1) minimizing the formation of iron oxides, such as the addition of complexing ligands and the inhibition of oxidation of ferrous ion by photoelectrons; (2) minimizing the deposition of iron oxides on the surface of ZVI, such as the supported ZVI composites, doped ZVI composites, and the premagnetization of ZVI. For example, in doped ZVI composites, when iron (anode) and second metal particles or carbon with higher potential (cathode) contacts, massive microscopic galvanic cells will be formed spontaneously between two electrodes. A relative potential difference drives the electron from iron to the doped metal or carbon before the adsorbed nitrate and proton accept electrons. Therefore, the nitrate reduction is mainly performed on the surface of second metal or carbon, which decreased the adverse effect of iron oxide on the surface of ZVI particles on nitrate reduction (Hosseini et al., 2011; Sparis et al., 2013).

In neutral condition, the way for accelerating the corrosion rate of iron may be as follows: (1) the formation of microscopic galvanic cells with ZVI as cathode, such as the addition of Cu^{2+} (Khalil et al., 2016b) and the doped ZVI composite. During the nitrate reduction by doped ZVI composite, a lot of microscopic galvanic cells are formed with ZVI as cathode. The relative potential difference can accelerate the corrosion of iron (Luo et al., 2014; Vilardi and Di Palma, 2017); (2) the increase of the surface of ZVI, such as nZVI or supported nZVI composites. As previously described, the activity of nZVI particles for nitrate reduction was higher than that of mZVI particles, and the activity of supported nZVI composites is higher than that of supported nZVI composites under the same reaction conditions.

In neutral condition, the reaction of mZVI with oxidant (Guo et al., 2015) or the addition of ferric or ferrous ions (Suzuki et al., 2012; Han et al., 2016) may be feasible for increasing the concentration of ferrous ion or surface associated Fe(II). Moreover, some non-ferrous reducing agents, such as H_2 (Hamid et al., 2015) or photoelectrons (Kobwittaya and Sirivithayapakorn, 2014), can provide synergistic effects with ZVI for the nitrate reduction in neutral condition.

4.3. Strategies of enhancing N_2 selectivity of nitrate reduction by ZVI

During the nitrate reduction by ZVI, the formation of intermediate nitrite is regard as a key step in determining the selectivity for N_2 and ammonia. Since the product of nitrite reduction by the surface of ZVI or Fe(II) was mainly ammonia, the inhibition of nitrite reduction to ammonia by ZVI surface or Fe(II) played a key role for enhancing N_2 selectivity of nitrate reduction. Therefore, the introduction of reductive species which can compete with ZVI surface or Fe(II) for converting nitrite to N_2 may be a passable solution for enhancing N_2 selectivity of nitrate reduction by ZVI. Taking doped ZVI composite for example, the galvanic couple can be formed between Fe and the second metal or carbon in the nitrate/doped ZVI composite system. Fe acted as anode, at which oxidation of Fe(0) to Fe(II) took place; while the doped metal or carbon served as cathode, at which nitrate reduction occurred. The adsorption performance and reduction rate of nitrate and proton, as well as the reduction of intermediate products on the doped metal or carbon, determined the reduction pathway and reduction end product (Zeng et al., 2017). For example, for (Pd—Cu)/nZVI system, a relative redox potential difference drove the electron from ZVI to Cu, and proton was transferred to the surface of Cu, which was then obtain electron from the surface of Cu to form Cu-H_{abs}. Nitrate was diffused and also adsorbed onto the surface of Cu, the adsorbed species [Cu–NO_{3ads}^{-}] could further reacted with Cu–H_{ads}. Oxygen atom in nitrate was then abstracted to form nitrite. The low affinity of Cu surface to nitrite led nitrite diffusing into solution (Sparis et al., 2013; Vilardi and Di Palma, 2017). Though the formed nitrite might be reduced to ammonia by ZVI surface or Fe(II), the formed nitrite could also migrated to the neighboring surface of Pd and further reacted with Pd–H_{ads} to form N_2, which increased the N_2 selectivity by 48% (Hamid et al., 2015).

In the nitrate/ZVI system, the simultaneous introduction of reductive species which can convert nitrite to N_2 and oxidative species which can oxidize Fe(II) may be also an efficient solution for increasing the N_2 selectivity of nitrate reduction. For example, Zhang et al. (2019) synthesized a novel Cu_2O-Cu^0@Fe^0 composite using mZVI sheets as substrate materials and used for nitrate reduction, combining with HCOOH under UV radiation. In Cu_2O-Cu^0@Fe^0/HCOOH/UV-A system, nitrate was firstly reduced to nitrite by the synergistic effect of species, such as e^- from the galvanic cell, $CO_2^{\bullet-}$, photoelectron, and so on. Nitrite was further reduced quickly to N_2 by $CO_2^{\bullet-}$. The further reduction of nitrite to ammonia did not proceed because the reduction rate of nitrite to N_2 by $CO_2^{\bullet-}$ was far higher than that of nitrite to ammonia by ZVI surface or Fe(II), as well as the nitrite reduction by Fe(II) was inhibited due to that Fe(II) had to take part in the recombination of photoelectrons and holes, which led to high N_2 selectivity of 95% (Fig. 4).

For another instance of TiO_2/ZVI composite, the nitrate reduction by TiO_2/ZVI composite under UV irradiation consisted of the following steps: (1) the generation of photoelectrons and holes through exciting TiO_2 by UV irradiation (Doudrick et al., 2013); (2) the transport of photoelectrons to ZVI due to the higher electron affinity than that of TiO_2, which acted as electron sink (Kobwittaya and Sirivithayapakorn, 2014); (3) nitrate was reduced to nitrite by photoelectrons on the surface of ZVI, or by electron released directly from ZVI (Liu et al., 2014); and (4) the formed nitrite was reduced to N_2 by H_2 produced from the action of holes and H_2O, which increased N_2 selectivity (Pan et al., 2012; Krasae and Wantala, 2016). The nitrite reduction to ammonia by ZVI surfaces or Fe(II) was weakened due to the competition of photoelectrons and holes for ZVI surfaces and Fe(II). Some scholars argued that high N_2 selectivity in the TiO_2/ZVI/UV system could be attributed to the maintenance of high level of ferrous ions due to its reducing condition (Pan et al., 2012). However, why the maintenance of high level of ferrous ions affected the nitrogen gas selectivity, is required for further investigation.

5. Concluding remarks and perspectives

5.1. Concluding remarks

ZVI as a reactive metal has been widely used for the reduction of nitrate due to its high efficiency, non-toxicity, low price and abundance. The performance of ZVI for the reduction of nitrate is affected by the physical characteristics of ZVI, such as its size, specific surface area, morphology, which are determined by their synthetic methods. The optimization of the ZVI performance can be obtained by modifying the morphology and structure of ZVI. However, what is the optimal particle size, specific surface area, shape or morphology of ZVI for maximizing nitrate reduction, is still unclear. Some operational parameters, such as solution pH, temperature, concentrations of DO, concentrations of nitrate and other water quality constituents, could also affect nitrate reduction by ZVI. Thus, the optimization of operational parameters is needed in order to increase the removal efficiency of nitrate. Even so, high nitrate reduction efficiency is always obtained at acid solution because the reduction of nitrate by ZVI often accompanied by the corrosion of ZVI, and the formation of iron oxide under neutral or alkaline conditions might inhibit the further reduction process. In order to overcome the shortcoming of the nitrate reduction in acid aqueous solution, such as inconvenient operation and the consumption of acid or alkali agent, more and more researches are focusing on the removal of nitrate with high efficiency by ZVI under near-neutral or neutral conditions.

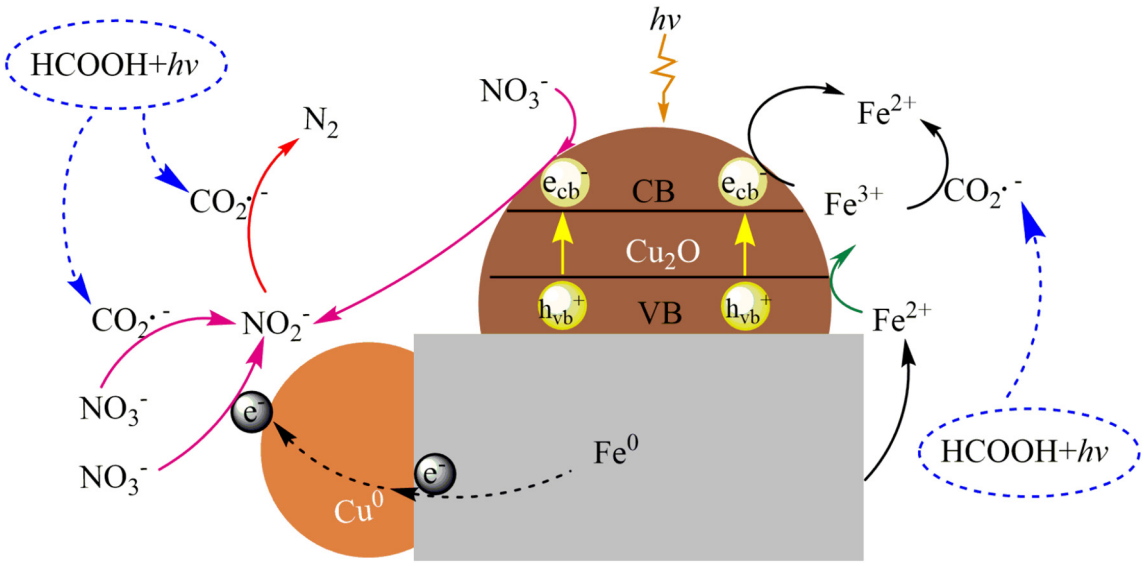

Fig. 4. Schematic representation of nitrate reduction Cu_2O-Cu^0@Fe^0 composite in the presence of formic acid and light (Zhang et al., 2019).

Two strategies have usually been used to increase the nitrate reduction efficiency of ZVI under near-neutral or neutral conditions. One is to increase the performance of ZVI composites by modifying their chemical composition and structure, the other is to optimize the reduction conditions. According to the corrosion electrochemistry theory, part of electron from ZVI as anode in galvanic cells during micro-electrolysis process will transfer to the cathode surface, resulting in the reduction of nitrate on the surface of cathode. Therefore, even if the passivation on the ZVI surface at neutral condition hinders electron transfer from the ZVI core, good reduction efficiency of nitrate could be gained by doped ZVI composites. As for the supported ZVI, the dispersion of supporter for the iron oxides and the buffer function for the acid and base is in favor of the high reduction efficiency of nitrate at neutral aqueous solution. Various support matrices were developed, such as rectorite, bentonite, palygorskite, silica materials, zeolite, porous carbon materials, resin, and exfoliated graphite, etc. The physical-chemical natures of the carrier (such as surface state, constituent, chemical stability, etc.) have great influence on the activity and nitrogen gas selectivity of supported ZVI composites. The nitrate reduction by the premagnetized ZVI or ZVI composites can be high efficiency because the generated homogeneous magnetic field and Lorentz force can promote the mass transfer process and corrosion of iron.

The optimization of the reaction conditions includes the addition of assistants in ZVI-nitrate system. These assistants include metal cations, organic or inorganic ligands, H_2 and light, etc. In the system of ZVI-nitrate with addition of assistant, besides the contribution of ZVI to the reduction of nitrate, other reducers also play an important role in the reduction of nitrate. The addition of metal cations, such as Fe^{2+}, Fe^{3+}, Al^{3+}, or Cu^{2+}, etc. can accelerate the corrosion of iron surface by buffering pH of the system or forming electrochemical reactions or improving the composition and structure of iron oxides; The ligands can eliminate iron oxide precipitates from the surface of ZVI by the complexation with Fe(II)/Fe(III); H_2 can accelerate kinetic reaction rate of nitrate by nZVI through preventing the formation of iron oxide layer. High reduction efficiency was obtained by Cu–Pd/nZVI composite combined with H_2 while H_2 supply in the presence of nZVI alone did not significantly increase nitrate removal due to a lack of adsorption of H_2 to Fe sites. The furtherance of light for the nitrate reduction always requires TiO_2/ZVI composite as reducer because the formation of oxidation species of iron was prevented by the role of photo-generated electrons and H_2 from the reaction between TiO_2 and light.

5.2. Challenges and future prospects

The desired reduction of nitrate by ZVI should be the high reduction efficiency of nitrate and high selectivity of nitrogen gas for nitrate reduction under a wide range of pH condition, especially under neutral condition. As previously mentioned, many methods were developed to enhance nitrate reduction/conversion and the kinetics by ZVI under neutral condition. However, the products of nitrate reduction by ZVI reactions were ammonia, nitrite, and nitrogen gas. Nitrogen gas is the desired end product, and nitrite concentration can be maintained at a lower concentration via slightly increasing the dosage of nZVI or reaction time. However, ammonia generation is still a problem during the nitrate reduction by ZVI. As well known, ammonia itself is a water pollutant, which is needed to be concerned. Some strategies have been developed to remove ammonia from the nitrate reduction system, such as using zeolite derivatives or stripping under the basic condition. However, future researches should be devoted to the exploration of new ZVI composites that improve the desirable end-product (nitrogen gas) selectivity during reduction of nitrate. As abovementioned, Cu–Pd/nZVI composite combined with H_2 and TiO_2/ZVI composite combined with light could increase the nitrogen gas selectivity, although the nitrogen gas selectivity is still low (below 85%). ZVI composite combined with other reducers could increase the nitrogen gas selectivity. Therefore, future efforts should be committed to further optimize the structure and composition of ZVI composite by developing new preparation method and to combine ZVI composite with other reducer in order to increase the nitrogen gas selectivity of nitrate reduction.

The application of ZVI and ZVI-based materials for the nitrate reduction in real water is still a great challenge. Although nitrate reduction by ZVI and ZVI-based materials has been widely investigated in aqueous solution, a few studies reported the nitrate reduction by ZVI and ZVI-based materials in actual water and wastewater, such as groundwater, industrial wastewater, the contaminated river water, and so on. Three issues must be faced when ZVI and ZVI-based materials was used for nitrate reduction in actual water: (1) pH control. Many real wastewater are in neutral pH condition. It is a problem to sustain the reactivity of ZVI for a longer period of time at neutral pH condition. Some strategies, such as the combination of micro-scale ZVI particles with granular ferric hydroxide (Song et al., 2013), iron nanoparticles synthesized by green tea and eucalyptus leaves (Wang et al., 2014) and Fe(0)/magnetite nanoparticles entrapped in Ca-alginate beads (Cho et al., 2015), were

proposed to reduce nitrate in actual water without pH control; (2) the fluctuations and complexity of actual water compositions, which can restrain the activity of ZVI particles. The addition of copper ions during the treatment could counteract the retardation effect and greatly enhanced the nitrate reduction (Khalil et al., 2018); and (3) Ammonia maybe generated during the process of nitrate reduction, which is also a pollutant, may pose a threat to human health and ecosystem. How to improve the N_2 selectivity of nitrate reduction is most important problem for practical application of ZVI-based materials for the nitrate reduction in real water and wastewater.

Acknowledgement

The research was financially supported by the National Natural Science Foundation of China (51878427), the Educational Commission of Sichuan Province of China (18ZA0397) and the Key Laboratory of Special Waste Water Treatment, Sichuan Province Higher Education System (SWWT2016-1).

References

Ahn, S., Oh, J., Sohn, K., 2001. Mechanistic aspects of nitrate reduction by Fe(0) in water. J. Korean Chem. Soc. 45, 395–398.
Ahn, S.C., Oh, S., Cha, D.K., 2008. Enhanced reduction of nitrate by zero-valent iron at elevated temperatures. J. Hazard. Mater. 156, 17–22.
Alowitz, M.J., Scherer, M.M., 2002. Kinetics of nitrate, nitrite, and Cr(VI) reduction by iron metal. Environ. Sci. Technol. 36, 299–306.
Anbia, M., Kamel, L., 2018. Preparation of pyramids structured silicon as a support for nanosized zero valent iron particles for nitrate removal from water. Silicon 10, 1851–1859.
Cai, X., Gao, Y., Sun, Q., Chen, Z., Megharaj, M., Naidu, R., 2014. Removal of co-contaminants Cu (II) and nitrate from aqueous solution using kaolin-Fe/Ni nanoparticles. Chem. Eng. J. 244, 19–26.
Chen, S.S., Hsu, H.D., Li, C.W., 2004. A new method to produce nanoscale iron for nitrate removal. J. Nanopart. Res. 639–647.
Chen, Y., Li, C., Chen, S., 2005. Fluidized zero valent iron bed reactor for nitrate removal. Chemosphere 59, 753–759.
Cheng, I.F., Muftikian, R., Fernando, Q., Korte, N., 1997. Reduction of nitrate to ammonia by zero-valent iron. Chemosphere 35, 2689–2695.
Cho, D., Chon, C., Jeon, B., Kim, Y., Khan, M.A., Song, H., 2010. The role of clay minerals in the reduction of nitrate in groundwater by zero-valent iron. Chemosphere 81, 611–616.
Cho, D., Song, H., Kim, B., Schwartz, F.W., Jeon, B., 2015. Reduction of nitrate in groundwater by Fe(0)/magnetite nanoparticles entrapped in Ca-alginate beads. Water Air Soil Pollut. 226, 206.
Choe, S., Chang, Y.Y., Hwang, K.Y., Khim, J., 2000. Kinetics of reductive denitrification by nanoscale zero-valent iron. Chemosphere 41, 1307–1311.
Choi, J., Sang, W.S.S., Choi, S.J., Kim, Y.H., 2008. Reductive denitrification using zero-valent iron and bimetallic iron. Environ. Technol. 30, 939–946.
Dong, L., Lin, L., Li, Q., Huang, Z., Tang, X., Wu, M., Li, C., Cao, X., Scholz, M., 2018. Enhanced nitrate-nitrogen removal by modified attapulgite-supported nanoscale zero-valent iron treating simulated groundwater. J. Environ. Manag. 213, 151–158.
Doudrick, K., Yang, T., Hristovski, K., Westerhoff, P., 2013. Photocatalytic nitrate reduction in water: managing the hole scavenger and reaction by-product selectivity. Appl. Catal. B Environ. 136-137, 40–47.
Eljamal, R., Eljamal, O., Khalil, A.M.E., Sahac, B.B., Matsunagaa, N., 2018. Improvement of the chemical synthesis efficiency of nano-scale zero-valent iron particles. J. Environ. Chem. Eng. 6, 4727–4735.
Ensie, B., Samad, S., 2014. Removal of nitrate from drinking water using nanoSiO_2-FeOOH-Fe core-shell. Desalination 347, 1–9.
Ezzatahmadi, N., Ayoko, G.A., Millar, G.J., Speight, R., Yan, C., Li, J., Li, S., Zhu, J., Xi, Y., 2017. Clay-supported nanoscale zero-valent iron composite materials for the remediation of contaminated aqueous solutions: a review. Chem. Eng. J. 312, 336–350.
Fan, X.M., Guan, X.H., Ma, J., Ai, H.Y., 2009. Kinetics and corrosion products of aqueous nitrate reduction by iron powder without reaction conditions control. J. Environ. Sci. 21, 1028–1035.
Fateminia, F.S., Falamaki, C., 2013. Zero valent nano-sized iron/clinoptilolite modified with zero valent copper for reductive nitrate removal. Process. Saf. Environ. Prot. 91, 304–310.
Frost, R.L., Xi, Y.F., He, H., 2010. Synthesis, characterization of palygorskite supported zero-valent iron and its application for methylene blue adsorption. J. Colloid Interface Sci. 341, 153–161.
Ghosh, N., Mandal, B.K., Mohan Kumar, K., 2012. Magnetic memory effect in chelated zero valent iron nanoparticles. J. Magn. Magn. Mater. 3839–3841.
Ghosh, A., Dutta, S., Mukherjee, I., Biswas, S., Chatterjee, S., Rajnarayan, S., 2017. Template-free synthesis of flower-shaped zero-valent iron nanoparticle: role of hydroxyl group in controlling morphology and nitrate reduction. Adv. Powder Technol. 28, 2256–2264.
Guo, X., Yang, Z., Liu, H., Lv, X., Tu, Q., Ren, Q., Xia, X., Jing, C., 2015. Common oxidants activate the reactivity of zero-valent iron (ZVI) and hence remarkably enhance nitrate reduction from water. Sep. Purif. Methods 146, 227–234.
Guo, J., Guo, P., Yu, M., Sun, Z., Li, P., Yang, T., Liu, J., Zhang, L., 2018. Chemical reduction of nitrate using nanoscale bimetallic iron/copper particles. Pol. J. Environ. Stud. 27, 2023–2028.
Hamid, S., Bae, S., Lee, W., Amin, M.T., Alazba, A.A., 2015. Catalytic nitrate removal in continuous bimetallic Cu-Pd/nanoscale zerovalent iron system. Ind. Eng. Chem. Res. 54, 6247–6257.
Han, L., Yang, L., Wang, H., Hu, X., Chen, Z., Hu, C., 2016. Sustaining reactivity of Fe^0 for nitrate reduction via electron transfer between dissolved Fe^{2+} and surface iron oxides. J. Hazard. Mater. 308, 208–215.
Hao, S., Zhang, H., 2017. High catalytic performance of nitrate reduction by synergistic effect of zero-valent iron (Fe^0) and bimetallic composite carrier catalyst. J. Clean. Prod. 167, 192–200.
Hao, Z.W., Xu, X.H., Jin, J., He, P., Liu, Y., Wang, D.H., 2005a. Science letters: simultaneous removal of nitrate and heavy metals by iron metal. J. Zhejiang. Univ-Sci. B 6, 307–310.
Hao, Z.W., Xu, X.H., Wang, D.H., 2005b. Reductive denitrification of nitrate by scrap iron filings. J. Zhejiang. Univ-Sci. B (6), 182–186.
Hosseini, S.M., Tosco, T., 2015. Integrating NZVI and carbon substrates in a non-pumping reactive wells array for the remediation of a nitrate contaminated aquifer. J. Contam. Hydrol. 179, 182–195.
Hosseini, S.M., Ataie-Ashtiani, B., Kholghi, M., 2011. Nitrate reduction by nano-Fe/Cu particles in packed column. Desalination 276, 214–221.
Hosseini, S.M., Tosco, T., Ataie-Ashtiani, B., Simmoms, C.T., 2018. Non-pumping reactive wells filled with mixing nano and micro zero-valent iron for nitrate removal from groundwater: vertical, horizontal, and slanted wells. J. Contam. Hydrol. 210, 50–64.
Hsieh, W., Pan, J.R., Huang, C., Su, Y., Juang, Y., 2010. Enhance the photocatalytic activity for the degradation of organic contaminants in water by incorporating TiO_2 with zero-valent iron. Sci. Total Environ. 408, 672–679.
Huang, Y.H., Zhang, T.C., 2002. Kinetics of nitrate reduction by iron at near neutral pH. J. Environ. Eng. 604–611.
Huang, Y.H., Zhang, T.C., 2004. Effects of low pH on nitrate reduction by iron powder. Water Res. 38, 2631–2642.
Huang, Y.H., Zhang, T.C., 2005a. Effects of dissolved oxygen on formation of corrosion products and concomitant oxygen and nitrate reduction in zero-valent iron systems with or without aqueous Fe^{2+}. Water Res. 39, 1751–1760.
Huang, Y.H., Zhang, T.C., 2005b. Enhancement of nitrate reduction in Fe^0-packed columns by selected cations. J. Environ. Eng. 131, 603–611.
Huang, Y.H., Zhang, T.C., 2006. Nitrite reduction and formation of corrosion coatings in zero valent iron systems. Chemosphere 64, 937–943.
Huang, C.P., Wang, H.W., Chiu, P.C., 1998. Nitrate reduction by metallic iron. Water Res. 32, 2257–2264.
Huang, Y.H., Zhang, T.C., Shea, P.J., Comfort, S.D., 2003. Effects of oxide coating and selected cations on nitrate reduction by iron metal. J. Environ. Qual. (4), 1306–1315.
Hwang, Y.H., Kim, D.G., Ahn, Y.T., Moon, C.M., Shin, H.S., 2010. Fate of nitrogen species in nitrate reduction by nanoscale zero valent iron and characterization of the reaction kinetics. Water Sci. Technol. 61, 705–712.
Hwang, Y., Kim, D., Shin, H., 2011. Mechanism study of nitrate reduction by nano zero valent iron. J. Hazard. Mater. 185, 1513–1521.
Ji, M., Ahn, Y., Khan, M.A., Abou-Shanab, R.A.I., Cho, Y., Choi, J., Kim, Y.J., Song, H., Jeon, B., 2011. Removal of nitrate and ammonium ions from livestock wastewater by hybrid systems composed of zerovalent iron and adsorbents. Environ. Technol. 32, 1851–1857.
Jiang, Z., Lv, L., Zhang, W., Du, Q., Pan, B., Yang, L., Zhang, Q., 2011. Nitrate reduction using nanosized zero-valent iron supported by polystyrene resins: role of surface functional groups. Water Res. 45, 2191–2198.
Jiang, Z., Zhang, S., Pan, B., Wang, W., Wang, X., Lv, L., Zhang, W., Zhang, Q., 2012. A fabrication strategy for nanosized zero valent iron (nZVI)-polymeric anion exchanger composites with tunable structure for nitrate reduction. J. Hazard. Mater. 233-234, 1–6.
Jiang, Z., Zhou, H., Chen, C., Wei, S., Zhang, W., 2015. The enhancement of nitrate reduction by supported Pd-Fe nanoscale particle. Sci. Adv. Mater. 7, 1734–1740.
Kamarehie, B., Aghaalib, E., Musavic, S.A., Hashemid, S.Y., Jafari, A., 2018. Nitrate removal from aqueous solutions using granular activated carbon modified with iron nanoparticles. Int. J. Eng. 31, 554–563.
Kapoor, A., Viraraghavan, T., 1997. Nitrate removal from drinking water-review. J. Environ. Eng. 123, 371–380.
Kassaee, M.Z., Motamedi, E., Mikhak, A., Rahnemaie, R., 2011. Nitrate removal from water using iron nanoparticles produced by arc discharge vs. reduction. Chem. Eng. J. 166, 490–495.
Khalil, A.M.E., Eljamal, O., Amen, T.W.M., Sugihara, Y., Matsunaga, N., 2016a. Optimized nano-scale zero-valent iron supported on treated activated carbon for enhanced nitrate and phosphate removal from water. Chem. Eng. J. 309, 349–365.
Khalil, A.M.E., Eljamal, O., Jribi, S., Matsunaga, N., 2016b. Promoting nitrate reduction kinetics by nanoscale zero valent iron in water via copper salt addition. Chem. Eng. J. 287, 367–380.
Khalil, A.M.E., Eljamal, O., Saha, B.B., Matsunaga, N., 2018. Performance of nanoscale zero-valent iron in nitrate reduction from water using a laboratory-scale continuous-flow system. Chemosphere 197, 502–512.
Kim, H., Kim, T., Ahn, J., Hwang, K., Park, J., Lim, T., Hwang, I., 2012. Aging characteristics and reactivity of two types of nanoscale zero-valent iron particles (FeBH and FeH_2) in nitrate reduction. Chem. Eng. J. 197, 16–23.
Kim, D., Hwang, Y., Shin, H., Ko, S., 2016. Kinetics of nitrate adsorption and reduction by nano-scale zero valent iron (NZVI): effect of ionic strength and initial pH. KSCE J. Civ. Eng. 20, 175–187.

Kobwittaya, K., Sirivithayapakorn, S., 2014. Photocatalytic reduction of nitrate over Fe-modified TiO_2. APCBEE Procedia 10, 321–325.

Krajangpan, S., Bermudez, J.J.E., Bezbaruah, A.N., Chisholm, B.J., Khan, E., 2008. Nitrate removal by entrapped zero-valent iron nanoparticles in calcium alginate. Water Sci. Technol. 58, 2215–2222.

Krasae, N., Wantala, K., 2016. Enhanced nitrogen selectivity for nitrate reduction on Cu-nZVI by TiO_2 photocatalysts under UV irradiation. Appl. Surf. Sci. 380, 309–317.

Lee, C.S., Gong, J., Huong, C.V., Oh, D.S., Chang, Y.S., 2016. Macroporous alginate substrate-bound growth of Fe0 nanoparticles with high redox activities for nitrate removal from aqueous solutions. Chem. Eng. J. 298, 206–213.

Li, J., Li, Y., Meng, Q., 2009. Removal of nitrate by zero-valent iron and pillared bentonite. J. Hazard. Mater. 174, 188–193.

Li, P., Lin, K., Fan, Z., Wang, K., 2017. Enhanced nitrate removal by novel bimetallic Fe/Ni nanoparticles supported on biochar. J. Clean. Prod. 151, 21–33.

Li, X., Zhou, M.H., Pan, Y.W., Xu, L., 2017. Pre-magnetized Fe^0/persulfate for notably enhanced degradation and dechlorination of 2,4-dichlorophenol. Chem. Eng. J. 1092–1104.

Li, Y., Fu, F., Ding, Z., 2018. Removal of nitrate from water by acid-washed zero-valent iron/ferrous ion/hydrogen peroxide: influencing factors and reaction mechanism. Water Sci. Technol. 77, 525–533.

Li, J., Shi, Z., Ma, B., Zhang, P., Jiang, X., Xiao, Z.X., 2019. Improving the reactivity of zerovalent iron by taking advantage of its magnetic memory: implications for arsenite removal. Environ. Sci. Technol. 10581–10588.

Lin, H., Chen, Y., Li, C., 2003. The mechanism of reduction of iron oxide by hydrogen. Thermochim. Acta 400, 61–67.

Liou, Y.H., Lo, S.L., Lin, C.J., H, K.W., Weng, C.S., 2005a. Chemical reduction of an unbuffered nitrate solution using catalyzed and uncatalyzed nanoscale iron particles. J. Hazard. Mater. 127, 102–110.

Liou, Y.H., Lo, S.L., Lin, C.J., H, K.W., Weng, C.S., 2005b. Effects of iron surface pretreatment on kinetics of aqueous nitrate reduction. J. Hazard. Mater. 126, 189–194.

Liou, Y.H., Lin, C.J., Weng, S.C., Ou, H.H., Lo, S.L., 2009. Selective decomposition of aqueous nitrate into nitrogen using iron deposited bimetals. Environ. Sci. Technol. 43, 2482–2488.

Liou, Y.H., Lin, C.J., Hung, I.C., Chen, S.Y., Lo, S.L., 2012. Selective reduction of NO_3^- to N_2 with bimetallic particles of Zn coupled with palladium, platinum, and copper. Chem. Eng. J. 181-182, 236–242.

Liu, H.B., Chen, T.H., Chang, D.Y., Chen, D., Liu, Y., He, H.P., Yuan, P., Frost, R., 2012. Nitrate reduction over nanoscale zero-valent iron prepared by hydrogen reduction of goethite. Mater. Chem. Phys. 133, 205–211.

Liu, Y., Lee, J., Zhao, Y., Zhang, M., Wang, L., Duan, Q., 2014. A novel preparation approach and denitrification performance of TiO_2/Fe^0 photocatalysts. Desalin. Water Treat. 57, 3125–3131.

Lu, H., Wang, J., Ferguson, S., Wang, T., Bao, Y., Hao, H., 2016. Mechanism, synthesis and modification of nano zerovalent iron in water treatment. Nanoscale 8, 9962–9975.

Lubphoo, Y., Chyan, J.M., Grisdanurak, N., Liao, C., 2015. Nitrogen gas selectivity enhancement on nitrate denitrification using nanoscale zero-valent iron supported palladium/copper catalysts. J. Taiwan Inst. Chem. Eng. 57, 143–153.

Lubphoo, Y., Chyan, J.M., Grisdanurak, N., Liao, C.H., 2016. Influence of Pd-Cu on nanoscale zero-valent iron supported for selective reduction of nitrate. J. Taiwan Inst. Chem. Eng. 59, 285–294.

Lucchetti, R., Onotri, L., Clarizia, L., Natale, F.D., Somma, I.D., Andreozzi, R., Marotta, R., 2017. Removal of nitrate and simultaneous hydrogen generation through photocatalytic reforming of glycerol over "in situ" prepared zero-valent nano copper/P25. Appl. Catal. B Environ. 202, 539–549.

Luo, J., Song, G., Liu, J., Qian, G., Xu, Z.P., 2014. Mechanism of enhanced nitrate reduction via micro-electrolysis at the powdered zero-valent iron/activated carbon interface. J. Colloid Interface Sci. 435, 21–25.

Ma, L., He, H., Zhu, R., Zhu, J., Mackinnon, I.D.R., Xi, Y.F., 2016. Bisphenol A degradation by a new acidic nanozero-valent iron diatomite composite. Catal. Sci.Technol. 6, 6066–6075.

Muradova, G.G., Gadjieva, S.R., Di Palma, L., Vilardi, G., 2016. Nitrates removal by bimetallic nanoparticles in water. Chem. Eng. Trans. 47, 205–210.

Pan, J.R., Huang, C., Hsieh, W., Wu, B., 2012. Reductive catalysis of novel TiO_2/Fe^0 composite under UV irradiation for nitrate removal from aqueous solution. Sep. Purif. Technol. 84, 52–55.

Ramavandi, B., Mortazavi, S.B., Moussavi, G., Khoshgard, A., Jahangiri, M., 2011. Experimental investigation of the chemical reduction of nitrate ion in aqueous solution by Mg/Cu bimetallic particles. React. Kinet. Mech. Catal. 102, 313–329.

Ren, Y., Zhou, J., Lai, B., Tang, W., Zeng, Y., 2016. Fe^0 and Fe^0 fully covered with Cu^0 (Fe^0 +Fe/Cu) in fixed bed reactor for nitrate removal. RSC Adv. 6, 1–34.

Ren, Y., Yang, J., Li, J., Lai, B., 2017. Strengthening the reactivity of Fe^0-(Fe-Cu) by premagnetization-implications for nitrate reduction rate and selectivity. Chem. Eng. J. 330, 813–822.

Rodríguez-Maroto, J.M., García-Herruzo, F., García-Rubio, A., Gómez-Lahoz, C., Vereda-Alonso, C., 2009. Kinetics of the chemical reduction of nitrate by zero-valent iron. Chemosphere 74, 804–809.

Ruangchainikom, C., Liao, C., Anotai, J., Lee, M., 2006. Effects of water characteristics on nitrate reduction by the Fe^0/CO_2 process. Chemosphere 63, 335–343.

Ryu, A., Jeong, S., Jang, A., Choi, H., 2011. Reduction of highly concentrated nitrate using nanoscale zero-valent iron: effects of aggregation and catalyst on reactivity. Appl. Catal. B Environ. 105, 128–135.

Sá, J., Agüera, C.A., Gross, S., Anderson, J.A., 2009. Photocatalytic nitrate reduction over metal modified TiO_2. Appl. Catal. B Environ. 85, 192–200.

Salam, M.A., Fageeh, O., Al-Thabaiti, S.A., Obaid, A.Y., 2015. Removal of nitrate ions from aqueous solution using zero-valent iron nanoparticles supported on high surface area nanographenes. J. Mol. Liq. 212, 708–715.

Shaban, Y.A., El Maradny, A.A., Al-Farawati, R.K., 2016. Photocatalytic reduction of nitrate in seawater using C/TiO_2 nanoparticles. J. Photochem. Photobiol. A 328, 114–121.

Shen, Z.Q., Wang, J.L., 2011. Biological denitrification using cross-linked starch/PCL blends as solid carbon source and biofilm carrier. Bioresour. Technol. 102 (19), 8835–8838.

Shi, Z., Nurmi, J.T., Tratnyek, P.G., 2011. Effects of nano zero-valent iron on oxidation–reduction potential. Environ. Sci. Technol. 45, 1586–1592.

Shi, J., Yi, S., He, H., Long, C., Li, A., 2013. Preparation of nanoscale zero-valent iron supported on chelating resin with nitrogen donor atoms for simultaneous reduction of Pb^{2+} and NO_3. Chem. Eng. J. 230, 166–171.

Shi, L., Du, J., Chen, Z., Megharaj, M., Naidu, R., 2014. Functional kaolinite supported Fe/Ni nanoparticles for simultaneous catalytic remediation of mixed contaminants (lead and nitrate) from wastewater. J. Colloid Interface Sci. 428, 302–307.

Shi, J., Long, C., Li, A., 2016. Selective reduction of nitrate into nitrogen using Fe–Pd bimetallic nanoparticle supported on chelating resin at near-neutral pH. Chem. Eng. J. 286, 408–415.

Shubair, T., Eljamal, O., Khalil, A.M.E., Matsunaga, N., 2018. Multilayer system of nanoscale zero valent iron and Nano-Fe/Cu particles for nitrate removal in porous media. Sep. Purif. Technol. 193, 242–254.

Shukla, A., Pande, J.V., Bansiwal, A., Osiceanu, P., Biniwale, R.B., 2009. Catalytic hydrogenation of aqueous phase nitrate over Fe/C catalysts. Catal. Lett. 131, 451–457.

Siantar, D.P., Schreier, C.G., Su, C., Chou, M., 1996. Treatment of 1,2-dibromo-3-chloropropane and nitrate-contaminated water with zero-valent iron or hydrogen/palladium catalysts. Water Res. 30, 2315–2322.

Singh, K.P., Singh, A.K., Gupta, S., 2012. Optimization of nitrate reduction by EDTA catalyzed zero-valent bimetallic nanoparticles in aqueous medium. Environ. Sci. Pollut. Res. 19, 3914–3924.

Sohn, K., Kang, S.W., Ahn, S., Woo, M., Yang, S., 2006. Fe(0) nanoparticles for nitrate reduction: stability, reactivity, and transformation. Environ. Sci. Technol. 40, 5514–5519.

Song, H.C., Jeon, B.H., Chon, C.M., Kim, Y.J., Nam, I.H., Schwartz, F.W., Cho, D.W., 2013. The effect of granular ferric hydroxide amendment on the reduction of nitrate in groundwater by zero-valent iron. Chemosphere 93, 2767–2773.

Song, X., Chen, Z., Wang, X., Zhang, S., 2017. Ligand effects on nitrate reduction by zero-valent iron: role of surface complexation. Water Res. 114, 218–227.

Sparis, D., Mystrioti, C., Xenidis, A., Papassiopi, N., 2013. Reduction of nitrate by copper-coated ZVI nanoparticles. Desalin. Water Treat. 51, 2926–2933.

Stefaniuk, M., Oleszczuk, P., Ok, Y.S., 2016. Review on nano zero valent iron (nZVI) from synthesis to environmental applications. Chem. Eng. J. 287, 618–632.

Su, C., Puls, R.W., 2004. Nitrate reduction by zero valent iron: effects of formate, oxalate, citrate, chloride, sulfate, borate, and phosphate. Environ. Sci. Technol. 38, 2715–2720.

Su, Y., Adeleye, A.S., Huang, Y., Sun, X., Dai, C., Zhou, X., Zhang, Y., Keller, A.A., 2014. Simultaneous removal of cadmium and nitrate in aqueous media by nanoscale zero valent iron (nZVI) and Au doped nZVI particles. Water Res. 63, 102–111.

Sun, Z., Zheng, S., Ayoko, G.A., Frost, R.L., Xi, Y.F., 2013. Degradation of simazine from aqueous solutions by diatomite-supported nanosized zero-valent iron composite materials. J. Hazard. Mater. 263, 768–777.

Suzuki, T., Moribe, M., Oyama, Y., Niinae, M., 2012. Mechanism of nitrate reduction by zero-valent iron: equilibrium and kinetics studies. Chem. Eng. J. 183, 271–277.

Tang, C., Zhang, Z., Sun, X., 2012. Effect of common ions on nitrate removal by zero-valent iron from alkaline soil. J. Hazard. Mater. 231-232, 114–119.

Teng, W., Bai, N., Liu, Y., Liu, Y., Fan, J., Zhang, W., 2017. Selective nitrate reduction to dinitrogen by electrocatalysis on nanoscale iron encapsulated in mesoporous carbon. Environ. Sci. Technol. 52, 230–236.

Tugaoen, H.O., Garcia-Segura, S., Hristovski, K., Westerhoff, P., 2017. Challenges in photocatalytic reduction of nitrate as a water treatment technology. Sci. Total Environ. 599-600, 1524–1551.

Vilardi, G., Di Palma, L., 2017. Kinetic study of nitrate removal from aqueous solutions using copper-coated iron nanoparticles. Bull. Environ. Contam. Toxicol. 98, 359–365.

Wang, J.L., Bai, Z.Y., 2017. Fe-based catalysts for heterogeneous catalytic ozonation of emerging contaminants in water and wastewater. Chem. Eng. J. 312, 79–98.

Wang, J.L., Chu, L.B., 2016. Biological nitrate removal from water and wastewater by solid-phase denitrification process. Biotechnol. Adv. 34, 1103–1112.

Wang, W., Jin, Z., Li, T., Zhang, H., Gao, S., 2006. Preparation of spherical iron nanoclusters in ethanol-water solution for nitrate removal. Chemosphere 65, 1396–1404.

Wang, T., Lin, J., Chen, Z., Megharaj, M., Naidu, R., 2014. Green synthesized iron nanoparticles by green tea and eucalyptus leaves extracts used for removal of nitrate in aqueous solution. J. Clean. Prod. 83, 413–419.

Wang, L., Zhou, H., Liu, J., Chen, J., Wei, S., Jiang, Z., 2018. Effect of humic acid on the nitrate removal by strong base anion exchanger supported nanoscale zero-valent iron composite. Water Air Soil Pollut. 229.

Westerhoff, P., James, J., 2003. Nitrate removal in zero-valent iron packed columns. Water Res. 37, 1818–1830.

Williams, A.G.B., Scherer, M.M., 2004. Spectroscopic evidence for Fe(II)-Fe(III) electron transfer at the iron oxide-water interface. Environ. Sci. Technol. 38, 4782–4790.

Wu, J.L., Yin, Y.N., Wang, J.L., 2018. Hydrogen-based membrane biofilm reactors for nitrate removal from water and wastewater. Int. J. Hydrog. Energy 43, 1–15.

Xi, Y.F., Megharaj, M., Naidu, R., 2011. Dispersion of zerovalent iron nanoparticles onto bentonites and use of these catalysts for orange II decolourisation. Appl. Clay Sci. 53, 716–722.

Xi, Y.F., Sun, Z.M., Hreid, T., Ayoko, G.A., Frost, R.L., 2014. Bisphenol A degradation enhanced by air bubbles via advanced oxidation using in situ generated ferrous ions from nanozero-valent iron/palygorskite composite materials. Chem. Eng. J. 247, 66–74.

Xiong, Z., Zhao, D., Pan, G., 2009. Rapid and controlled transformation of nitrate in water and brine by stabilized iron nanoparticles. J. Nanopart. Res. 11, 807–819.

Xu, J., Hao, Z., Xie, C., Lv, X., Yang, Y., Xu, X., 2012. Promotion effect of Fe^{2+} and Fe_3O_4 on nitrate reduction using zero-valent iron. Desalination 284, 9–13.

Yang, G.C.C., Lee, H., 2005. Chemical reduction of nitrate by nanosized iron: kinetics and pathways. Water Res. 39, 884–894.
Yang, Z., Shan, C., Mei, Y., Jiang, Z., Guan, X., Pan, B., 2018. Improving reductive performance of zero valent iron by H_2O_2/HCl pretreatment: a case study on nitrate reduction. Chem. Eng. J. 334, 2255–2263.
Yun, Y., Li, Z., Chen, Y., Saino, M., Cheng, S., Zheng, L., 2018. Elimination of nitrate in secondary effluent of wastewater treatment plants by Fe^0 and Pd-Cu/diatomite. J. Water Reuse Desalin. 8, 29–37.
Zaidi, N.S., Sohaili, J., Muda, K., Sillanpää, M., 2013. Magnetic field application and its potential in water and wastewater treatment tystems. Sep. Purif. Rev. 43, 206–240.
Zawaideh, L.L., Zhang, T.C., 1998. The effects of pH and addition of an organic buffer (HEPES) on nitrate transformation in Fe^0-water systems. War. Sci. Tech. 38, 101–107.
Zeng, Y., Walker, H., Zhu, Q., 2017. Reduction of nitrate by NaY zeolite supported Fe, Cu/Fe and Mn/Fe nanoparticles. J. Hazard. Mater. 324, 605–616.
Zhang, F., Jin, R., Chen, J., Shao, C., Gao, W., Li, L., Guan, N., 2005. High photocatalytic activity and selectivity for nitrogen in nitrate reduction on Ag/TiO_2 catalyst with fine silver clusters. J. Catal. 232, 424–431.
Zhang, H., Jin, Z., Han, L., Qin, C., 2006. Synthesis of nanoscale zero-valent iron supported on exfoliated graphite for removal of nitrate. Trans. Nonferr. Metal. Soc. 16, s345–s349.
Zhang, J., Hao, Z., Zhang, Z., Yang, Y., Xu, X., 2010. Kinetics of nitrate reductive denitrification by nanoscale zero-valent iron. Process. Saf. Environ. Prot. 88, 439–445.
Zhang, Y., Li, Y., Li, J., Hu, L., Zheng, X., 2011. Enhanced removal of nitrate by a novel composite: nanoscale zero valent iron supported on pillared clay. Chem. Eng. J. 171, 526–531.
Zhang, Y., Douglas, G.B., Pu, L., Zhao, Q., Tang, Y., Xu, W., Luo, B., Hong, W., Cui, L., Ye, Z., 2017. Zero-valent iron-facilitated reduction of nitrate: chemical kinetics and reaction pathways. Sci. Total Environ. 598, 1140–1150.
Zhang, D., Wang, B., Gong, X., Yang, Z., Liu, Y., 2019. Selective reduction of nitrate to nitrogen gas by novel Cu_2O-Cu^0@Fe^0 composite combined with HCOOH under UV radiation. Chem. Eng. J. 359, 1195–1204.
Zhao, W., Zhu, X., Wang, Y., Ai, Z., Zhao, D., 2014. Catalytic reduction of aqueous nitrates by metal supported catalysts on Al particles. Chem. Eng. J. 254, 410–417.
Zhao, Y., Cao, X., Song, X., Zhao, Z., Wang, Y., Si, Z., Lin, F., Chen, Y., Zhang, Y., 2018. Montmorillonite supported nanoscale zero-valent iron immobilized in sodium alginate (SA/Mt-NZVI) enhanced the nitrogen removal in vertical flow constructed wetlands (VFCWs). Bioresour. Technol. 267, 608–617.